UNIVERSITAT POLITÈCNICA DE VALÈNCIA

ESCUELA TÉCNICA SUPERIOR INGENIERÍA INDUSTRIAL VALENCIA

INDUSTRIAL ENGINEERING MASTER THESIS

ANALYSIS AND MODELLING OF ALUMINIUM MATRIX COMPOSITES REINFORCED WITH INTERMETALLICS

AUTHOR: Antoine LEJEUNE

SUPERVISOR: David Jerónimo BUSQUETS MATAIX

CO - TUTOR: Alina Iuliana PRUNA

Academic year: 2020-21

Agradecimientos

En primer lugar, quiero agradecer al Profesor David Busquets Mataix, mi tutor de este proyecto. En el proceso de realización, me dio muchos consejos e ideas, que han sido de gran ayuda a la hora de realizar el trabajo.

También quiero dar las gracias al profesor Ferhun Cem Caner Baskurt, catedrático en la Universitat Politècnica de Catalunya, por sus consejos muy preciosos para la modelación informática con el software Abaqus, pero también por estos cursos de modelación informática que tuve la suerte de seguir durante un semestre. Quiero agradecer también al Profesor Luis Miguel Llanes Pitarch, también catedrático en la Universitat Politècnica de Catalunya, por sus cursos de tecnologías de materiales compuestos de matriz inorgánica.

De manera más general, quiero agradecer a todos los profesores que he tenido, tanto en la universidad como fuera de ella, por haber fomentado, aunque algunos más que otros, el desarrollo de mi curiosidad en el ambiente de la ingeniería de materiales.

Por último, pero no por ello menos importante, un agradecimiento a mis compañeros de la Universidad de Lorena que siempre me han apoyado, que sea por problemas de modelación, de redacción del informe o simplemente por haberme dedicado su tiempo. Un agradecimiento especial a mis amigos, Alberto y Gemma, por su ayuda a lo largo de este semestre, tanto con respecto a los trámites administrativos de la Universitat Politècnica de València, como para la elaboración de ese trabajo de fin de máster. Una vegada més, moltes gràcies a vosaltres !

Abstract

Since the last two decades, metal matrix composites (MMC) have emerged as an important class of high performances materials for use in aerospace, automobile, chemical and transportation industries because of their improved strength, high elastic modulus, density, thermal and electrical properties and increased wear resistance over conventional base alloy. With the aim of reducing the environmental impact since manufacture processes to the step of recycling, those materials have generated interest among the scientific community for those exceptional properties that promised the development of ever more efficient materials.

The purpose of this Master's thesis is to focus on the modelling of thermal and mechanical behaviours of aluminium matrix composites reinforced with intermetallics such as TiB_2, ZrB_2 or CrB_2 thanks to the software ABAQUS FEA®(Dassault Systèmes).

To carry out this mechanical study, two parameters were considered: the volume content of particles and the properties of reinforcements. For the thermal study, coefficients of thermal expansion were estimated of a composite material reinforced with TiB_2 at a certain volume fraction, and thermal behaviours of several configurations of reinforcements were studied. A whole model has been created thanks to ABAQUS FEA®, to simulate the mechanical behaviour of an aluminium based metal matrix composite by applying a normal displacement on the surface of the specimen.

As expected, the results revealed that by increasing elastic properties of intermetallics, we also increased elastic properties of the composites. It has been shown that the Young modulus of the whole material increases linearly with the volume fraction of particulates. Finally, the thermal study shown that the reinforcement of a specimen of aluminium with intermetallics improves the refractory behaviour of the material, but it also depends of their dispersion into the matrix. About coefficients of thermal expansion, reinforcing a material with low-CTE material compared to the matrix reduces expansion properties of the composite material, whether in axial or transverse direction.

The perspectives of this work would be to change the type of mechanical loads and try to study the material behaviour by applying dynamic mechanical loads. Also, properties of wear resistance could be simulated by implementing an explicit model on ABAQUS. FEA®. Behaviours of such materials could also be studied at high temperature, for which elastic and thermal properties may change.

Key words: Metal-based matrix composite materials, aluminium alloy, intermetallics, analysis, finite element method, modelling, Abaqus, short-fibers, particles, Newton's law, rule of mixture, elastic behaviours.

Resumen

A lo largo de los veinte últimos años, los materiales compuestos de matriz metálica (MMC) han aparecido como un tipo de material muy interesante con propiedades de alta eficacidad empleados en los campos aeroespacial, automóvil, químico, y de la industria de transporte gracias a su mayor resistencia a rotura, su alto modulo de elasticidad, su densidad, sus propiedades eléctricas y térmicas, y su mayor resistencia al desgaste respeto a las aleaciones metálicas convencionales. Con el objetivo de reducir el impacto ambiental desde los procesos de fabricación hasta el paso del reciclaje, estos materiales han generado interés entre la comunidad científica por aquellas propiedades excepcionales que ya prometían el desarrollo de materiales cada vez más eficientes.

El propósito de este trabajo de fin de máster es centrarse en la modelización del comportamiento térmico y mecánico de materiales compuestos con matriz de aluminio y reforzados con intermetálicos como TiB_2, ZrB_2 or CrB_2 gracias al software ABAQUS FEA®(Dassault Systèmes).

Para llevar al cabo este estudio mecánico, se consideraron dos parámetros: el porcentaje de partículas, y la naturaleza y propiedades de los refuerzos. Para el estudio térmico, se calculó el coeficiente de dilatación térmica según la dirección axial pero también transversal con un material reforzado con TiB_2. También se estudiaron comportamientos térmicos de varias configuraciones de refuerzos al aplicar un flujo de calor en una pared del material. Se ha creado un modelo completo gracias al software ABAQUS FEA®, para simular el comportamiento mecánico de un material compuesto de matriz metálica de aluminio mediante la aplicación de un desplazamiento normal en la superficie de la muestra.

Como se esperaba, los resultados mostraron que al aumentar las propiedades elásticas de los intermetálicos, también aumentamos las propiedades elásticas de los compuestos. Se ha demostrado que el módulo Young del composite aumenta linealmente con el porcentaje de partículas, en dirección axial pero también transversal. Finalmente, el estudio térmico mostró que el refuerzo de una muestra de aluminio con intermetálicos mejora el comportamiento refractario del material, pero también depende de su dispersión dentro de la matriz. En cuanto a los coeficientes de expansión térmica, el refuerzo de un material con un material de bajo coeficiente de dilatación térmica en comparación con la matriz reduce las propiedades de expansión del material compuesto, ya sea en dirección axial o transversal.

El futuro de ese trabajo podría ser cambiar el tipo de cargas mecánicas e intentar estudiar el comportamiento del material aplicando cargas mecánicas dinámicas. Además, las propiedades de la resistencia al desgaste podrían simularse mediante la aplicación de un modelo explícito en ABAQUS FEA®.

Palabras claves: Materiales compuestos de matriz metálica, aleación de aluminio, intermetálicos, análisis, modelización, método de los elementos finitos, Abaqus, fibras cortas, partículas, ley de Newton, ley de la mezcla, comportamientos elásticos.

Resum

Al llarg dels vint últims anys, els materials compostos de matriu metàl·lica (MMC) han aparegut com un tipus de material molt interessant amb propietats d'alta eficàcia empleats en els camps de l'enginyeria aeroespacial y de l'automòbil, de la industria química, i de la indústria del transport gràcies a la seua major resistència a ruptura, el seu alt mòdule d'elasticitat, la seua densitat, les seues propietats l'elèctriques i tèrmiques, i la seua millor resistència al desgast respecte als aliatges metàl·lics convencionals. Amb l'objectiu de reduir l'impacte ambiental des dels processos de fabricació el reciclatge, estos materials han generat un gran interès a la comunitat científica, per aquelles propietats excepcionals que ja prometien el desenvolupament de materials cada vegada més eficients.

L'objectiu d'aquest treball fi de màster es centra en la modelització del comportament tèrmic y mecànic dels materials compostos amb matriu d'alumini i reforçats amb compostos intermetàl·lics com el TiB2, ZrB2 o CrB2 gràcies al programari ABAQUS FEA (Dassault Systems). Per a portar a terme aquest estudi mecànic s'han considerat dos paràmetres: el percentatge de partícules, la seua natura i les propietats dels reforços. Per a l'estudi tèrmic s'ha considerat el coeficient de dilatació lineal segons les direccions axial i transversal amb un material reforçat amb TiB2. També s'estudiaren els comportaments tèrmics de varies configuracions de reforços al aplicar un flux de calor a una de les parets del material. S'ha creat un model complet gràcies al programari ABAQUS FEA per a simular el comportament metàl·lic d'un material d'alumini mitjançant l'aplicació d'un desplaçament normal a la superfície de la mostra.

Com era d'esperar, els resultats mostraren que al augmentar les propietats elàstiques dels materials intermetàl·lics, també es milloren les propietats elàstiques dels MMC. També s'ha demostrat que el mòdul de Young del material augmenta linealment amb el percentatge de partícules tant en direcció axial com en direcció transversal. Finalment l'estudi tèrmic demostrà que el reforç d'una mostra d'alumini amb compostos intermetàl·lics milloren el comportament refractari del material depenent de la seva dispersió dins del material. Respecte al coeficient de dilatació tèrmica, el reforç d'una matriu amb un material de baix coeficient de dilatació lineal respecte al de la matriu, redueix les propietats de dilatació del material compost tant en direcció axial o en direcció transversal.

L'estudi portat a terme en aquest present treball fi de màster podria ampliar-se aplicant càrregues mecàniques dinàmiques. A més, les propietats de la resistència al desgast podrien simular-se mitjançant l'aplicació d'un model explícit amb el ABAQUS FEA.

Paraules claus: Materials compostos de matriu metàl·lica, aliatge d'alumini, intermetàl·lics, anàlisi, modelització, mètode dels elements finits, Abaqus, fibres curtes, partícules, llei de Newton, llei de la mescla, comportaments elàstics.

Contents

List of Figures

List of Tables

Glossary

AMMC Aluminium metal matrix composite. 23

B.C Before Christ. 10

CMC Ceramic matrix composite. 18, 20

CTE Coefficient of thermal expansion. 2, 8, 17, 29, 33, 34, 40, 42

FEA Finite element analysis. 27, 29

IRM Inverse rule of mixture. 33, 36, 38, 39

MMC Metal matrix composite. 2, 3, 7, 10, 11, 18–20, 23, 25

PMC Polymer matrix composite. 18, 19

ROM Rule of mixture. 17, 33, 36, 38, 40, 42

1 Introduction

1.1 The need of composite materials

The use of composite materials is not something recent. The earliest usage of composites is credited to the Mesopotamian. These ancient people used to glue wood strips at different angles in order to create stuffs like plywood in 3400 B.C. Furthermore, between 2181 and 2055 B.C Egyptian people designed death masks as shown in figure 1 made of cartonnage and layers of linen or papyrus soaked in plaster. Around the 1500's B.C, Egyptians and Mesopotamian settlers used a mixture composed of mud and straw to create strong and durable buildings. Even back then, the high potential of those materials had been considered and largely exploited. The times B.C marked the beginning of types of composites materials used in daily applications[1][2]

From the ancient times, builders, artisans, engineers, manufacturers and other trades and crafts kept going to develop composites of a wider array of materials for even more sophisticated applications. From the 1870's through the 1890's, a chemical revolution has changed composite development.

Figure 1: Rear of a cartonnage Anubis mask, Ptolemaic era. [3]

The modern era of composites did not begin until scientists developed plastics. In the early 1900's, chemical advances led to the development of plastics. Materials such as vinyl, polystyrene, phenolic and polyester were developed and reinforcement was needed to improve strength and rigidity. Until then, natural resins derived from plants and animals were the only source of glues and binders. These scientific advances in the field of polymer matrix composites constitute the first generation of advances of composite materials.[1][2][4]

The second generation started by the end of World War II when a small niche of composites industry was in full swing. This new generation was characterized by the launch of Soviet satellite Sputnik in 1957 that was a major event in the history of MMC.This marked the beginning of "Space

Race" between the world super powers. Spacecrafts had to be built with lighter materials than metal alloys and stronger than polymer composites to carry payload to space breaking the gravitational grip and also resisting the high temperatures that sometimes went up to 1500 °C during reentry of the spacecraft into the atmosphere. It was during this period that scientists started to look at metal matrix composites as a possibly solution. Before this development, little works were already provide in this field to reinforce copper with steel reinforcement wires. The space race also inspired scientists and innovators to develop carbon and boron fibers whose properties matched up with their expectations.

Once the race to the moon over, scientists started thinking of re-usable space craft like MIR spacecraft from the Union of Soviet Socialist Republics, Skylab, and the Space Shuttle since 1970. Due to the fact that spacecraft are subject to repeated temperature variations, scientists were forced to investigate to materials that have the combination of properties like high stiffness and strength, high temperature resistance and low coefficient of thermal expansion so that the material will not contract and deform too much during the thermal cycling periods. Boron filament, the first high-strength and high-modulus reinforcement, was developed both for metal and organic matrix composites and coatings for those fibers made them possible for metallic matrices.

Nowadays, the major obstacle for metal matrix composites which prevents their entry into fast moving consumer markets is their cost. An example that can be cited is the area of sports equipment, where Duralcan®(Al reinforced with 10% Al_2O_3 particulates) and Al reinforced with 20% SiC particulates are used in bicycle frames to reduce weight and improve strength. They are of high cost and used in high performance mountain bikes.[5][2][6]

Since their beginnings, composites research has attracted subventions from governments, manufacturers and universities. These investments allowed investigations to accelerate. Specialized companies, such as aerospace composite companies, has found a place in the industry. Two applications that continue to experience innovative growth are airplane composite materials and composite sheets for marine use. Other materials such as environmentally-friendly resins incorporating recycled plastics and bio-based polymers are still in high demand for stronger, lighter and environmentally friendly products. Looking ahead, the development of fibers and resins will create even more applications for everyday and specialized use.

Obviously, the rapid growth of the technology in industries is linked with the need to use lightweight materials that fulfill industrial and environmental criteria with advantageous mechanical and tribological characteristics. Gradual advancements in manufacturing technologies of materials made possibilities of creation of lightweight MMCs for different applications at lower costs with higher quality.

A good future can be predicted for these composite classes, as the industries have focused on obtaining low-cost and high-performances MMCs. Therefore the research must expand through leaps and bounds.[5][7]

1.2 Mechanical behaviours of composites materials

1.2.1 Definition and characteristics

A structural composite is a material system consisting of two or more phases on a macroscopic scale, whose mechanical performances and properties are designed to be superior to those of the constituent materials acting independently. When they are combined they create a material specialised to do a certain job, for instance to become stronger, lighter or resistant to thermal gradients. They can also improve strength and stiffness. The reason for their use over traditional materials is because they improve the properties of their base materials and are applicable in many situations. One of the phases is typically discontinuous, stiffer, and stronger and it is what we call the reinforcement, whereas the less stiff and weaker phase is continuous and called the matrix. Sometimes, because of chemical interactions, manufacture, or other processing effects, an other distinct phase called an interphase exists between the reinforcement and the matrix. Figure 2 depicts those different phases of a composite materials.

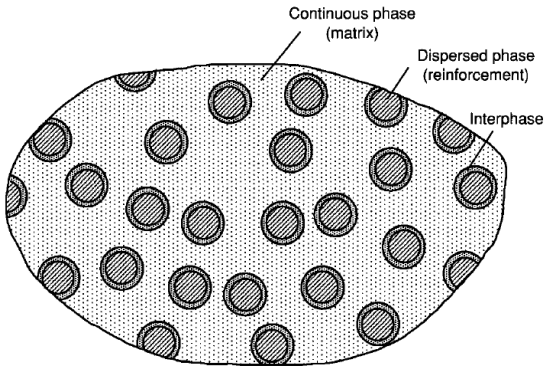

Figure 2: Phases of a composite material. [8]

The mechanical behaviours of a two-phase composite system depend mostly on the filler characteristics such as, the geometry of inclusions, their size, the size distribution, the orientation of inclusions, the filler volume fraction, the relative positions between these inclusions, the physical state of the filler, but also on the matrix characteristics. The more nonuniform the reinforcement distribution, the more heterogeneous the material, and the higher the scatter in properties and the probability of failure in the weakest areas. [8][9][6]

The phases of a composite material system play different roles, which compensate for each other and depend on the type and application of the composite material. In the case of low and medium performance materials, the reinforcement use to be in the form of short fibers or particles and may increase stiffness of the material. The matrix, on the other hand, is the main load bearing constituent which governs the mechanical properties of the material. In the case of high-performance structural composites, the normally continuous fiber reinforcement constitutes the backbone of the

material, which determines its stiffness and strength in the fiber direction or principal direction. The matrix phase also provides an important protection for the sensitive fibers, bonding, support, and local stress transfer from one fiber to another to overcome the mechanical fragility of the matrix. The interphase, even if it's small in dimensions, plays an important role in controlling the failure mechanisms, failure propagation, and the overall stress-strain behavior to failure of the material.[6]

Although they at first appeared to have only advantages, as time has passed and as investigations has evolved, multiple characterization tests have shown weak points in these materials, for example, the resistance to inter laminar fracture in a material constituted from the stacking of different layers. Therefore, the mechanical characterization of composites, their improvement, their weak points, and the way in which they can be overcome, are considered as interesting points.[8]

1.2.2 Basic concepts, geometry and physical properties

Composite materials have many mechanical behaviour characteristics that are mostly different from those of more conventional engineering materials as metals or polymers. Some of those characteristics are merely modifications of conventional behaviour, while others are totally new and require new analytical and experimental procedures. Most common engineering materials are both homogeneous (they have uniform properties, independently of the position in the body) and isotropic (their properties are the same in every direction at a point in the body).

In contrast, composite materials are often both heterogeneous and anisotropic, that is to say, a material whose properties are different in all directions at a point in the body. No plane of material properties symmetry exists. Some composite materials are typically complex, especially those with fibers placed at many angles in space. Because of the heterogeneity of composite materials, they are conveniently studied from two points of view: micro-mechanics and macro-mechanics, the most readily appreciated being macro-mechanic.[8][10]

In order to develop mechanical theories to model the behaviour of composite materials under stress or thermal gradient, some types of symmetries within the material have been considered to simplify analytical models, while getting as close as possible to reality. Throughout this study, the materials studied are considered as having fully-elastic and linear behaviours. As in the case of homogeneous and isotropic materials, the Hooke's law in equation 1 can be applied to composite materials, but in a generalized way, where σ represents the stress, E the Young's modulus and ε the strain.

$$\sigma = E\varepsilon \tag{1}$$

Considering a material with fully-elastic and linear behaviours, without any relation of symmetry, the Hooke's law can be adapted and the elastic constant E becomes a matrix as properties are not the same in all directions and points of the body. Thanks to symmetry relations of $\underline{\sigma}$ and $\underline{\varepsilon}$, we

find that $\sigma_{13} = \sigma_{31}$, $\sigma_{23} = \sigma_{32}$, $\sigma_{12} = \sigma_{21}$ and we obtain a 6x6 stiffness matrix $\underline{\underline{C}}$ which contains elastic properties of the composite materials in any direction and point of the body. This adapted Hooke's law is shown in equation 2.

$$\begin{pmatrix} \sigma_{11} \\ \sigma_{22} \\ \sigma_{33} \\ \sigma_{13} \\ \sigma_{23} \\ \sigma_{12} \end{pmatrix} = \begin{pmatrix} C_{11} & C_{12} & C_{13} & C_{14} & C_{15} & C_{16} \\ C_{21} & C_{22} & C_{23} & C_{24} & C_{25} & C_{26} \\ C_{31} & C_{32} & C_{33} & C_{34} & C_{35} & C_{36} \\ C_{41} & C_{42} & C_{43} & C_{44} & C_{45} & C_{46} \\ C_{51} & C_{52} & C_{53} & C_{54} & C_{55} & C_{56} \\ C_{61} & C_{62} & C_{63} & C_{64} & C_{65} & C_{66} \end{pmatrix} \cdot \begin{pmatrix} \varepsilon_{11} \\ \varepsilon_{22} \\ \varepsilon_{33} \\ \varepsilon_{13} \\ \varepsilon_{23} \\ \varepsilon_{12} \end{pmatrix} \tag{2}$$

Taking into account energetic criteria and considering an orthotropic material, i.e. a material whose properties are different in three mutually perpendicular directions at a point in the body and has three mutually perpendicular planes of material property symmetry, equation 2 can be modified and simplified as shown in equation 3. [6]

$$\begin{pmatrix} \varepsilon_{11} \\ \varepsilon_{22} \\ \varepsilon_{33} \\ \varepsilon_{13} \\ \varepsilon_{23} \\ \varepsilon_{12} \end{pmatrix} = \begin{pmatrix} 1/E_1 & -\nu_{21}/E_2 & -\nu_{31}/E_3 & 0 & 0 & 0 \\ -\nu_{12}/E_1 & 1/E_2 & -\nu_{32}/E_3 & 0 & 0 & 0 \\ -\nu_{13}/E_1 & -\nu_{23}/E_2 & 1/E_3 & 0 & 0 & 0 \\ 0 & 0 & 0 & 1/G_{23} & 0 & 0 \\ 0 & 0 & 0 & 0 & 1/G_{13} & 0 \\ 0 & 0 & 0 & 0 & 0 & 1/G_{12} \end{pmatrix} \cdot \begin{pmatrix} \sigma_{11} \\ \sigma_{22} \\ \sigma_{33} \\ \sigma_{13} \\ \sigma_{23} \\ \sigma_{12} \end{pmatrix} \tag{3}$$

As we can notice, an orthotropic composite material is defined by three Young's moduli, six Poisson's coefficients and three shear moduli. Obviously, in academic studies, cases are simpler and some approximations are considered. Generally, academic cases require knowledge of five elastic constants at most, this is particularly true for orthotropic materials with transverse isotropy.

However, this generalized Hooke's law only describes stress and strain states of a raw reinforced material, or a layer in case of a laminated composite material because of the discontinuity of stresses at the interface of each layer. If we wanted to study the mechanical behaviour of the whole laminated composite, we should apply Hooke's law to any layer. In order to determine the general behaviour of the superposition of a certain number of layers, some hypothesis has been developed at the beginning of the 20th century has the Love-Kirchhoff hypothesis, or the Reissner-Mindlin hypothesis.[6]

In order to illustrate the complexity of determining laws of elastic behaviour of composite materials, let's consider a simple case study shown in figure 3

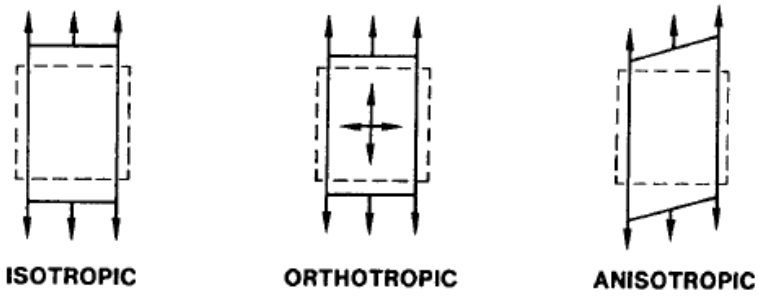

Figure 3: Mechanical behavior of various materials constrained. [10]

Dotted lines represent the initial shape of the material, before deformation and continuous lines the shape after deformation.

- For isotropic material, applying a normal stress causes extension in the direction of the stress and contraction in the perpendicular directions because of the volume conservation, but no shearing deformation. In this case, only two material properties, Young's modulus and Poisson's ratio are required to quantify the deformations.

- In the case of an orthotropic material, the application of normal stress in a principal material direction i.e. along one of the intersections of three orthogonal planes of material symmetry, results in extension in the direction of the stress and contraction perpendicular to the stress. The magnitude of this extension in principal direction under normal stress in that direction is different from the extension in another principal direction under the same normal stress in that other direction. In the case of laminated composites reinforced by fibers, one principal direction is superposed to the direction of orientation of the fibers. Thereby, Young's moduli exist in the various principal material directions. Because of different properties in the principal directions of the material, the contraction can be either more or less than the contraction of a similarly isotropic material loaded with the same elastic modulus in the direction of load. That's why different Poisson's ratios are associated with different pairs of principal material directions.

- For anisotropic material, application of a normal stress leads not only to extension in the direction of the stress and contraction perpendicular to it, but to shearing deformation because of coupling between loading modes inside the material and more specifically at the interface between reinforcement and matrix. In our case, normal load led to shear-extension coupling.[10]

Rule of mixture

Some rules has been established to predict various properties of a composite material made up of particles or continuous unidirectional fibers. It provides a theoretical upper and lower bound on properties of the material. These rules enable to predict properties such as Young's modulus, mass density, ultimate tensile strength or thermal and electrical conductivity. For material reinforced with continuous unidirectional fibers, the Voigt model, also called *linear mixture rule*, is usually employed for axial loading. This rule is based on the fact that if the material is to stay intact, the strain of the fibers, must equal the strain of the matrix. It hence gives the following relation:

$$E_{c,a} = V_r E_r + (1 - V_r) E_m \tag{4}$$

Where $E_{c,a}$ is the Young's modulus of the composite materials in the direction parallel to the fibers, E_r is the Young's modulus of the reinforcement, E_m the Young's modulus of the matrix, and V_r is the volume fraction of reinforcement.

For transverse loading, the Reuss-model, or *inverse mixture rule*, is usually employed to determine transverse properties whose mathematical expression is presented in equation 5.[11][12]

$$E_{c,t} = \frac{1}{\frac{V_r}{E_r} + \frac{1 - V_r}{E_m}} \tag{5}$$

Tsai-Halpin relation

It is well known that the predictions for transverse Young's modulus do not agree well with the experimental results. This establishes a need for better modeling techniques in order to refine the determination of transverse properties of composite materials. An advancement of these models, which is also applicable for short fibers or particles, is the model developed by Tsai and Halpin. This is a semi-empirical model that has been developed for design purposed, which can be used for a wide range of elastic properties and fiber volume fractions. This relation has been developed as simple equations by curve fitting to results that are based on elasticity. By implementing a geometry factor, which can be determined from fiber geometry, packing geometry and loading conditions, the geometry and the orientation of the reinforcement can be considered. The mathematical expression of Tsai-Halpin is shown in equation 6.[13]

$$E_{c,t} = \frac{1 + \zeta\eta.V_r}{1 - \eta.V_r} E_m \tag{6}$$

where η is constructed in such way that when $V_r \to 0$, $E_{c,t} \to E_m$, and when $V_r \to 1$, $E_{c,t} \to E_r$.

$$\eta = \frac{\frac{E_r}{E_m} - 1}{\frac{E_r}{E_m} + \zeta} \tag{7}$$

Where ζ is called the geometry factor and $E_{c,t}$ is the Young's modulus of the composite in the transverse direction. For example, for circular fibers in a packing geometry of a square array, ζ = 2. More generally, for a fiber of length a and width b, $\zeta = 2\frac{a}{b}$, where b is in the direction of loading.[12][13]

Since coefficient of thermal expansion (CTE) is different depending on the measuring direction, simple models have been developed in order to estimate the CTE of composite materials in principal directions based on the characteristics of the individual components. In 1968, Schapery [14] developed an analytical approach for calculating upper and lower bounds on thermal expansion coefficients of isotropic and anisotropic composites reinforced with fibers with isotropic phases. Equation 8 depicts the expression of the axial coefficient of thermal expansion of a composite material by Schapery.[11]

$$\alpha_{33c} = \frac{E_r \alpha_r . V_r + E_m \alpha_m . (1 - V_r)}{E_c} \tag{8}$$

Where α_{33c} represents the axial CTE of the composite, α_r and α_m the CTE of the reinforcement and the matrix respectively, and E_C the Young's modulus of the composite material in axial direction, that can be approach by ROM or using experimental value. Transverse CTE can also be determined based on the same model, supposing that the material is transversely isotropic, as shown in equation 9:

$$\alpha_{22c} = \alpha_{11c} = (1 + \nu_m)\alpha_m . (1 - V_r) + (1 + \nu_r)\alpha_r . V_r - \alpha_{33c}\nu_{31c} \tag{9}$$

With,

$$\nu_{31c} = \nu_r . V_r + \nu_m . (1 - V_r) \tag{10}$$

Where α_{22c} and α_{11c} are transverse CTEs, equal due to the hypothesis of a transversely isotropic material, $\nu_r$and ν_m are respectively Poisson's ratio of the reinforcement and the matrix, and ν_{31c} is the Poisson's ratio of the composite under axial loading in the plane (1;3).

As we could realised through this section, the mechanic of composite materials is something very complicated and sophisticated. That's why computer-assisted design software became very useful in the development of brand new materials. Through the following sections we will compare both computed results and analytical results based on rules developed above.

1.3 Materials used for composite materials

1.3.1 Materials used for matrix

As mentioned in 1.2.1, the main purpose of the matrix is to transfer the mechanical loads to the reinforcement. It also protects the reinforcement against various environmental conditions. However, due to thermal stability of some materials, we cannot use a matrix in any thermal conditions. Three families of composites are differentiated according to the nature of the matrix:

- Polymer matrix composites (PMC) which are by far the largest volumes today at industrial scale.
- Metal matrix composites (MMC).
- Ceramic matrix composites (CMC) for very high-end technical applications and working at high temperatures such as in space, nuclear and military areas, as well as braking area.

As figure 4 depicts, the choice of the constituent of the matrix depends on the operating temperature desired. Obviously, polymer components are those that can only used at low temperatures because of the low-melting temperature. At temperatures above 600°C, ceramic matrix are mainly employed because of their very high thermal stability. Some metallic alloys can also be used as matrix at high temperatures, but their manufacture remain generally very expensive.

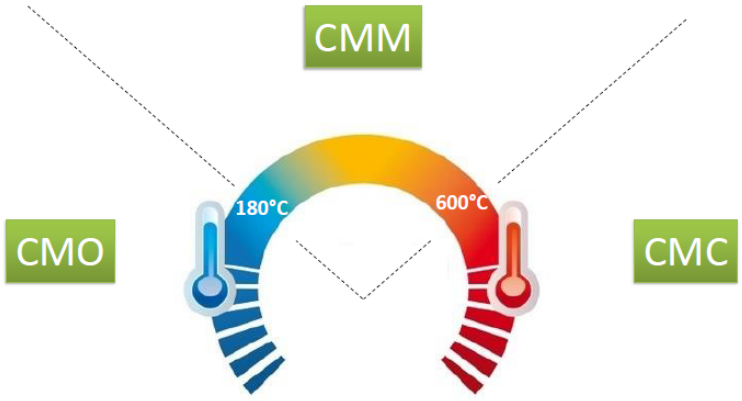

Figure 4: Illustration of the thermal areas of use of each type of matrix. [6]

Polymer matrix composites

In the case of PMC, two large families of matrices are distinguished: Thermosetting resins and thermoplastic resins. Thermosetting resins are in a viscous liquid state and are formed by initiating a chemical reaction of polymerization by adding a hardener, resulting in solidification, that is to say

that this reaction is an irreversible transformation. In Europe, thermosetting matrix composites represent 65% of all processed composites. Thermoplastic resins exist in solid state in form of pellets or plates, and formed by softening them by heating, and then solidifying them by cooling . This transformation is reversible, and this type of resin appeared later.[6][15]

Among the most well-known polymer matrices, there are unsaturated polyester resins that are quite cheap and mostly reinforced with glass fibers. They represent 90% of the market of polymer matrices. Epoxy resins are also well known because of their great mechanical behaviours. They are generally reinforced with carbon fibers for the construction of structural parts and aeronautic. However, this resin is five time more expensive than unsaturated polyester resins. About thermoplastic resins, the main resins utilized are polypropylene, polyamide, polyethylene, polyetherimide, polyphenylene sulfide and polyetheretherketone. They present good resistance to impact, unlimited retention but poor thermomechanical properties and high manufacturing cost.

PMCs are well-known for their quite low price and the easy method of production. Manufacturers of PMC can create cost-effective products with various manufacturing procedures. Polymers produce good components as they could be processed conveniently, and it represents an asset for these category of material.[16]

Metal matrix composites

In the case of MMCs, the composite material is composed of a metallic matrix as aluminium, magnesium, titanium, copper or nickel, and of a metallic or ceramic reinforcement as steel tires, silicon carbide particles, alumina, or diamond powder for example. The use of a metal matrix in a composite has several advantages compared to organic matrices. The most relevable is its thermal stability, allowing to push back the limits of use in engine environments or hyper-sonic structures. This class of matrix also improve ageing and fire resistance, ductility and gas tightness. In contrast, manufacture processes of MMC are generally more complex than those of PMC.

The most commons MMC are manufactured with an aluminium-alloy matrix due to its low density, good forming and joining properties and corrosion resistance. Composite based on titanium have also a vast application. Magnesium is the lightest out of a range of non-ferrous metals ans is generally used in electronics equipment. Copper-based composites also experiment a huge development thanks to their excellent wear resistance.

MMC are generally more expensive than the conventional materials they replace. So the performance gains really have to be important enough to justify the associated excess. Nowadays, they still occupy a small part in the industry (about 5000 tonnes/year) partly due to difficult manufacturing processes and the high cost of certain reinforcements.[17][6]

Ceramic matrix composites

CMC also called thermo-structural materials, are manufactured to work at very high temperatures. They are mainly used in the space industry, military and aeronautic fields, as well as for the design of high-end components such as brake discs or pads. The ceramic-based matrix materials are having exceptional corrosion resistance, high melting points, superior compressive strength, and stability at high temperatures. The main ceramic matrices employed are composed of silicon carbide, carbon or alumina.[18]

Even if MMCs are generally more expensive and difficult to manufacture than conventional materials, we will see later that their improved properties can motivate their development in many areas that require rigidity and resistance to thermal conduction.

1.3.2 Materials used for reinforcement

As it has been said in 1.2.1, there are two main families of reinforcement: Particles and fibers. We will divide this part into two sections in order to differentiate those two types of reinforcement.

Particles

Through the term of "particles", we can differentiate some categories of reinforcement as micro-beads, powders or nanoparticles. Generally, the properties of composite materials reinforced with particles are considered as isotropic due to the quasi-homogeneous distribution of particles. We designed by the term of particles all quasi-isotropic reinforcement morphologies, whose ratio length/diameter is about 0.2 to 1, that can be spherical or steel-like.[19][6] For particle reinforcements, the volume fractions generally vary between 10% and 50%. The average particle size can vary between 5 µm and 100 µm, depending on the supplier and the type of application envisaged.

Particles are generally used to improve features such as rigidity of the matrix, resistance to abrasion or temperature resistance. They are also often used to reduce the cost of the material.

Among the most well-known particle-reinforced composite materials, we have for example car tires whose matrix is made of rubber and reinforced by carbon particles to improve the strength and toughness of polymer matrix. The reinforcing effect principally depends on the size, shape, and dispersion of the particles in the matrix, as well as the interface adhesion between the particles and matrix.[20]

Another example, shown in figure 5, with a completely different manufacture process is that one of spheroidal steel.

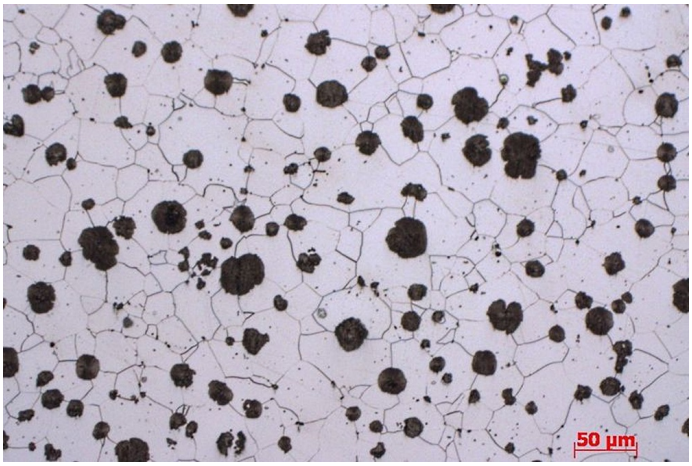

Figure 5: Microstructure of a spheroidal steel. [21]

Spheroidite forms when carbon steel is heated to 700 °C for over 30 hours. In our case, spheroidites are brittle cementite particles formed in a ductile ferrite matrix. The aim is to soften carbon steels and allow more formability. This is the softer form and more ductile steel. We notice in figure 5 that it results in a structure of rods or spheres of cementite within primary structure.

Obviously, there are still plenty of categories of particles used as reinforcement, but it would be convenient to focus on the categories and properties related to the subject of this master thesis. Subsequently, we will approach another type of particles on which will be based the simulations.

Fibers

A fiber is a solid, of which one of the dimensions is much larger than the other two. It consists of several threads. Among fibers, we can distinguish short-fibers, long-fibers, continuous fibers and whiskers. Continuous fibers have the same length as the piece. The length of a long-fiber is about 12 mm and can be up to the length of a continuous fiber. Short-fibers are ever shorter than 12 mm. Whiskers are mono crystalline discontinuous mineral fibers, and therefore have very high mechanical properties due to their structure. They have very small dimensions, with a diameter about 0.1 to 1 micron, and a length between 20 and 100 microns. They are almost flawless single crystals, especially without dislocations. Their modulus of elasticity is much larger than that of the material which composes them when it is in its ordinary form. Processes of elaboration of whiskers are based on epitaxial growth i.e. an oriented growth technique, with respect to each other, of two crystals with a certain number of symmetry element. This step of growth is initiated by a gas phase or by a pyrolysis of a precursor rich in silicon, that is very complicated to carry out. The handling of whiskers in divided state poses security problems because their inhalation is carcinogenic.[6]

Fibers can be divided into four classes due to their inherent nature. Among this, we have natural, synthetic, ceramic and metallic fibers. Among ceramic fibers, the most well-known are glass fibers.

In this section, we will focus on ceramic and metallic fibers because they are closest to our subject, although natural and synthetic fibers represent a large part of reinforcement used with polymer matrix.

Composite materials reinforced with glass fibers represent 90% of the world production of composites. This can be explained by their low cost of production, their corrosion resistance and their low thermal expansion. As mentioned in 1.1, boron were one of the first categories of fibers created in order to improve strength, thermal properties or ageing behaviours. However, due to its prohibitive cost of production, it has been gradually replaced by carbon fiber. Carbon fiber represent a major step forward in the development of composite materials. Those fibers are generally elaborated from an organic precursor called polyacrylonitrile. They exhibit a wide variety of properties of interest in order to improve behaviour of materials as its electric or thermal conductivity, thermal expansion or processability. Unfortunately, they still have prohibitive cost of production but the increase in production quantities sets out to reduce their price.[22]

Nowadays, metal fibers are widely produced and available in a wide range of different alloys and product forms due to the combination of properties such as high electrical conductivity, excellent high thermal corrosion resistance or electromagnetic/anti-static shielding. They may consist of different types of metals and alloys such as steel, nickel, copper or silver and are generally obtained through a step of wire-drawing.

For example, in a 7 kg-car tire, there are about 5 kg of rubber and 2 kg of steel wires used to reinforced the rubber. It allows better resistance to the load exerted by the car. The more these wires are, the more the tyre carcass is reinforced, which reduces the risk of a puncture.[23]

1.4 Aluminium-based metal matrix reinforced with intermetallics

In this section, we will focus on the material of interest for this study. After having discussed the wide variety of materials employed in the field of composite materials, their properties and challenges for their future development, we will focus on a composite with aluminium-based matrix, reinforced with particles of intermetallics.

1.4.1 Overview of characteristics of those materials

i Aluminium-based metal matrix

As said in 1.3.1, aluminium alloys are used extensively as composite material matrices due to the combination of outstanding mechanical properties, wear resistance, excellent ductility, good corrosion resistance, and easy availability. They have also easy-machinability and high-accessibility compared to other materials. They became highly acceptable materials for a broad array of applications also thanks to their flexibility in processing. Among MMCs, particulate reinforced aluminium matrix composite materials is the most important category. Due to those exceptional properties, aluminium-based metal matrix composite materials have been developed in a wide variety of sectors as show figure 6. As it has already been said in 1.1, the need to develop ever lighter materials for many reasons as fuel-consumption reduction or increase of resistance properties or economic reasons, for example, led scientists to employ aluminium matrix composites in more and more sectors as aircraft, aerospace, construction or marine industries, and it has been widely developed since.[15]

Figure 6: Various sectors of application of MMCs in industries. [15]

Different methods were adopted for large-scale production of AMMCs, but the liquid metallurgy way remains mostly used due to the facility of fabrication. Though the other ways of production were more efficient regarding to the properties reached and micro-structural features, the ease of fabrication and the cost economics made the liquid metallurgy way a competitive method for bigger sized components at large-scale production. In the last two decades, although research went on in the field of aluminium-base metal matrix, the results obtained have only confirmed the previous attained results. It is now considered that a plateau in the possible improvement of this class of matrix has been reached.[24]

ii Intermetallics used as reinforcements

First of all, it would be convenient to define the term of *intermetallic* in order to understand in a better way the content of the following sections. An intermetallic compound, or semi-metallic, is the association of metals or metalloids ,i.e. a chemical element with a large number of properties in common with metals and nonmetals, with each other by a chemical bond. Nowadays, there is still no standard definition of a metalloid, but in particularly, boron, silicon, germanium, arsenic, antimony and tellurium are mostly considered as metalloids by the scientific community.

Those intermetallic compounds exist for a specific composition or within a defined region of the phase diagram of the elements constituting it. They usually form an ordered structure, that is to say that each atom usually occupy specific sites of the lattice. They often offer a compromise between ceramic and metallic properties when hardness and resistance to high temperatures is important enough to put aside toughness and the ease of processing. they generally exhibit low density and good oxidation behaviour compared to usual metallic materials.[25][26]

Intermetallic properties are generally not in agreement with properties of elements they are composed of. This discontinuity of properties constitute the major difference between alloys and intermetallic compounds. Among the most well-known intermetallic compounds, the most important reinforcement candidates are titanium aluminides Ti_3Al and TiAl due to their low density and excellent mechanical properties, including at high temperatures. Al-based metal matrix composite materials reinforced with titanium aluminides are now substituted to nickel superalloys, resulting in important economy in weight. Moreover, aluminide reinforcement are in thermodynamic equilibrium with the matrix of aluminium, that is to say that there is a real chemical bond between both components.[27][28]

Through the following sections, we will consider three intermetallic compounds: titanium diboride TiB_2, zirconium diboride ZrB_2 and chromium diboride CrB_2. They are considered as ultra-refractory ceramics due to their very good thermal stability above 2000°C, their high melting point, but also to the iono-covalent nature of the bonds between atoms, although those atomic bonds are generally covalent rather than ionic because of the difference of electronegativity between atoms. Nevertheless, they have thermal conductivity a bit higher than conventional ceramic materials. The fact that these materials result of the combination of a metalloid and a metallic element makes that they are also considered as intermetallics.

1.4.2 Manufacture processes

The production of an aluminium-based metal matrix composite material reinforced with intermetallics can be conducted in two ways: in-situ or ex-situ.

Manufactures processes of metal matrix composite materials are quite often associated to a liquid state fabrication step. It involves incorporation of dispersed phase into a molten matrix metal, followed by its solidification. In order to provide high mechanical properties of the composite material, good interfacial bonding between the dispersed phase and the liquid matrix should be obtained. Wetting improvement may be achieved by coating the reinforcement. It not only reduces interfacial energy, but also prevents chemical interaction between the dispersed phase and the matrix. Their are various methods of liquid state fabrication of MMCs such as stir casting or infiltration like gas pressure infiltration, but the most popular is stir casting.[29]

Stir casting is the simplest and the most cost effective method of liquid state fabrication. The dispersed phase, i.e. reinforcement, is mixed to a molten matrix metal by means of mechanical stirring. After this stirring step, the liquid composite material is cast by conventional methods. However, the segregation of reinforcement particles and poor adhesion at the interface are normally observed with this method of fabrication. Thermodynamic instability is also something problematic with this technique.[29]

That's why since the early 1990's, in-situ techniques have been developed to fabricate Al–Si alloy-based metal matrix composites, which can lead to a better adhesion at interfaces between both components and hence improve mechanical properties thanks to an effective load transfer and a minimized wear rate.[30][31]

In-situ technique of fabrication of MMCs is a process which involves the synthesis of reinforcing phases directly within the matrix as a result of precipitation from the melt during its cooling and solidification. Subsequently, we will describe the manufacture process of aluminium-based MMC by in-situ techniques in the case of TiB_2 reinforcement. The process can be extended to ZrB_2 and CrB_2 as it is the same.

As said above, let's consider the synthesis of TiB_2. This in-situ synthesis can be carried out from different reactants, using different ways such as alloy-alloy technique or reactive hot pressing method. In another process, reactants such as pure aluminium and salts as potassium hexaflurotitanate K_2TiF_6 and potassium tetrafluroborate, carefully weighed as per stoichiometric equation, KBF_4 are melted at 850°C in an electric resistance furnace. Metal salts are blended and preheated for one hour at 250 °C before adding to the mixture at 850°C. The chemical equation is described below:

$$K_2TiF_{6(l)} + KBF_{4(l)} + Al_{(l)} \longrightarrow TiB_{2(inAlloy)} + KFAlF_{3(l)} + KF_{(l)} + AlF_{3(l)} \quad (11)$$

The Gibbs free-energy equation for reaction 11 was found to be: 981.990+112.8T J.mol^{-1}. This is an exothermic reaction favoured at lower temperatures.

The same reaction in order to produce ZrB_2 in alloy can be conducted by substituting K_2ZrF_6 for K_2TiF_6.[32]

In the system of equation 11, the formation of TiB_2 in alloy can be divided into three parts. The first one relates to the decomposition of metal salts to KF liquid, TiF_4 and BF_3 gases at the molten liquid interface to form TiB_2 and AlF_3. Then occurs the aluminothermic reduction of TiF_4 and BF_3 at the molten liquid metal interface to form TiB_2 and AlF_3 as shown in equation 12.[33]

$$TiF_{4(g)} + BF_{3(g)} + Al_{(l)} \longrightarrow TiB_{2(s)} + AlF_3 \quad (12)$$

After that, a cryolite is formed by a mixture of $KFAlF_3$ and KF. The liquid mixture is finally casted into steel mould preheated at 800°C and then air-cooled.[31] Studies of the microstructure of the composite material obtained shown that TiB_2 particles are distributed along the grain boundary regions, and very minimal agglomerations were observed. The fact that particles were distributed s along the grain boundaries indicates that particle segregation at the solid/liquid interface during solidification still exists. It has been proved that factors such as temperature or reaction holding time highly affects the mechanical properties of the final material.[32]

2 Objectives

The goal of this Master's thesis is to analyse and model the mechanical and thermal behaviours of an aluminium matrix composites reinforced with intermetallics. Due to the pandemic situation, I did not have access to the UPV laboratories, and the purpose of this project has been slightly modified. Initially, it was planned to deal with the in-deep characterization of an aluminium matrix composites reinforced with TiB_2, ZrB_2 or CrB_2 by different techniques such as microstructural analysis including high-resolution transmission electron microscopy, nanoindentation with special emphasis in the determination of the modulus of elasticity by ultrasonic techniques. However, we decided with my tutor David Busquets to stay on the idea of studying the mechanical and thermal properties of such a material.

In order to do so, the software Abaqus FEA®will be used carrying finite element analysis. Studies will be carried out to investigate the influence of various parameters such as the volume

fraction of reinforcement or the nature of the reinforcement and more specifically the influence of the properties of the components on the properties of the whole material. Thermal simulations will also be carried out in order to measure coefficients of thermal expansion of the composite material, but also to study the refractory behaviour of such a material. This would be the opportunity to show that FEA can conducts to an approximate information of the mechanical behaviour of a material without any lab experiment.

3 Materials and methods

In this part will be presented the software used for simulations. The material properties computed will also be presented as the methodology to implement computationally in order to simulate as well as possible the behaviours of a composite material.

3.1 Material data used for simulations

The specimen simulated is 0.3 mm in length, 0.3 mm height and 0.05 mm width as shown in figure 7. Such small dimensions are considered in order to get as close as possible to reality, to the dimensions of reinforcements in composite materials.

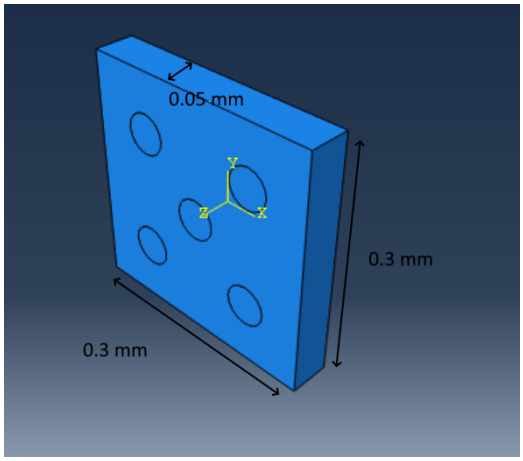

Figure 7: Figure of the dimensions of the specimen model with ABAQUS/FEA.

In figure 7, the reinforcement has a radius of 0.03 mm, or 30 µm. As we can see, the reinforcement has the shape of short-fibers with cylindrical shape. It was an easy way to design such a composite in two dimensions, and then extrude in the width.

In order to consider objects of the order of mm, and even of micron, dimensions were directly computed in mm and approximate size of the modeling space for the part definition has been set a 2 instead of 200 initially. Since Abaqus has no built-in system of units, all input data can be specified in consistent units, generally defined from length unit. Using mm unit for length, units of some data must be modified too as shown in table 1 to make the system consistent.

Table 1: Table of the consistent units of the system computed in ABAQUS/FEA.

Quantity	SI unit	SI (mm)
Length	m	mm
Force	N	N
Time	s	s
Temperature	K	K
Density	kg.m^{-3}	tonnes.mm^{-3}
Young's modulus	Pa	MPa
Specific heat capacity	J.kg^{-1}.K^{-1}	mJ.$tonnes^{-1}$.K^{-1}

It does not matter if thermal conductivity is specified in W.m^{-1}.K^{-1} or mW.mm^{-1}.K^{-1} because there is no multiplier factor that appears.

3.1.1 Material data for matrix

A 7075 aluminium alloy is used as matrix material. This is an aluminium alloy with excellent mechanical properties, good ductility, high strength, toughness and good resistance to fatigue. This alloy is one of the most commonly used aluminium alloy for highly stressed structural applications such as aircraft structural parts. Its chemical composition is shown below [34]:

Table 2: Table of the chemical composition of AA7075 (mass fraction, %).

Si	Fe	Cu	Mn	Mg	Cr	Ni	Zn	Ti	Al
≤ 0.1	0.19	1.53	≤ 0.1	2.55	0.18	≤ 0.1	5.89	≤ 0.1	Balance

The mechanical and thermal properties used are those of an AA7075-T6, which is an aluminium alloy 7075 that has been tempered. It is usually achieved by homogenizing the cast at 450 °C for a couple of hours, then quenching and ageing. Those properties are presented in the table below. Notice that they are not considered as temperature-dependant data because in the case of static analysis, temperature effects are not considered, and for thermal analysis, the variation of temperature is low enough to consider properties as constant in the interval of temperature computed. This will be explained in more details in the following sections. Properties presented below were measured at 293 K.[35]

Table 3: Table of the mechanical and thermal properties of the AA7075-T6 matrix.

Properties	AA7075-T6
Density (kg.m^{-3}) d	2805
Young's modulus (MPa) E	71
Poisson's coefficient ν	0.32
Thermal conductivity (W.m^{-1}.K^{-1}) k	196
CTE (K^{-1}) α	$2.4.10^{-5}$
Specific heat capacity (J.kg^{-1}.K^{-1}) C_p	860

3.1.2 Material data for reinforcements

As said in ii, three types of intermetallics are considered for simulations: TiB_2, ZrB_2 ans CrB_2. Only TiB_2 will be used for coupled thermal-displacement analysis, so only its thermal properties are needed. Scientists from the *Department of Materials Science and Engineering* of the Kyoto University and the *National Institute for Materials Science* of Namiki in Japan have investigated about the elastic constants and thermal expansivities of this three intermetallics in case of monocrystals [36]. Polycrystalline elastic constants were evaluated from the monocrystal elastic constants by Hill's method. Specific heat capacity, thermal conductivity and density of TiB_2 have been obtained thanks to the investigations of B. Basu, G. B. Raju and A. K. Suri [37] about the production submicrometre sized TiB_2 powders. Those properties are presented below:

Table 4: Table of the mechanical and thermal properties of TiB_2 ZrB_2 and CrB_2.

Properties	TiB_2	ZrB_2	CrB_2
Density (kg.m^{-3}) d	4520	/	/
Young's modulus (MPa) E	583.5	526	422.5
Poisson's coefficient ν	0.111	0.135	0.206
Thermal conductivity (W.m^{-1}.K^{-1}) k	80	/	/
CTE (K^{-1}) α	$6.35.10^{-6}$	/	/
Specific heat capacity (J.kg^{-1}.K^{-1}) C_p	554	/	/

3.2 The software ABAQUE FEA®

3.2.1 Generalities

ABAQUS FEA is a software for finite element analysis and computer-aided for engineering. ABAQUS product consists of five core software products, including ABAQUS/CAE. ABAQUS/CAE is a complete solution for Abaqus finite element modeling, visualization and process automation. The

intuitive interface integrates modeling, analysis, job management, and results visualization in a consistent, easy-to-use environment that is simple to learn for new users.[38]

To implement a model with ABAQUS/CAE, it is necessary to follow specific steps, depending on the type of procedure, that is to say the type of analysis to carry out. Generally, any modelling begin with the creation of the parts of the specimen. Then, sections with specific properties are assigned to the parts. After that, a step is created to implement the type of analysis to be performed. This is a basic concept of Abaqus that problem history is divided into steps, that is to say, into convenient phases of the material history. Optional history data, such as loads, boundary conditions, or output requests are also often computed. Generally, the last step is the structured meshing. This meshing step will define the quality of results. The finer the mesh, the more accurate the results. The different meshing techniques provide varying levels of automation and user control. In our case, the main issue is that with Abaqus student edition, the number of nodes is limited to 1000. It is therefore necessary to deal with the number of meshing element, their type of elements etc...

3.2.2 Computing parameters

Through this section will be presented the parameters computed for each analysis for a better understanding of the results. Mechanical and thermal analysis have steps in common such as the parts creation. As depicted in figure 8 matrix and reinforcement are created separately. In order to join this two parts, an assembly has been created and tie constraints have been applied between the internal surface of the holes of the matrix and the external surface of the reinforcement to transfer loads from the matrix to the reinforcement. These tie constraints make it possible to create a rigid body at the interface matrix/short-fibers.

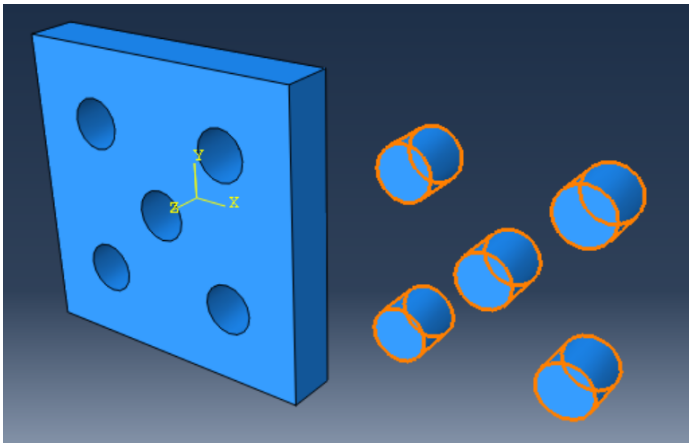

Figure 8: Figure of the two parts created in ABAQUS/FEA, the matrix on the left and the reinforcement on the right.

Further steps will be described subsequently in more details for each type of analysis carried out.

i Mechanical analysis

Two parameters were studied through mechanical analysis such as the influence of the volume fraction of reinforcement or the material used for reinforcement. For each case, analysis were conducted with displacement control. In our case, the stability of analysis would not be affected by load or displacement control because the materials studied are considered as having fully-elastic and linear behaviours, so no concept of yield stress are taken into account. In some cases, once yield limit crossed, the model diverges while applying load control. The displacement applied was about 0.0005 mm and it is constant throughout the simulations. This displacement has been applied to the specimen in ten equal increments. Axial and transverse moduli were measured as shown in figure 10 and figure 9 respectively. Thus, the displacement was apply along the x-axis for transverse analysis, and along the z-axis for axial analysis. Obviously, boundary conditions have been computed to obtain convergent results as shown in the two above figures to stop displacements along x,y and z-axis of the opposite face of that one where the displacement is applied.

As we only study the Young's modulus of composite material without taking into account time-dependent material effects as creep, swelling, viscoelasticity or inertia effects, a static general procedure has been conducted for a time period of 1 second. Only Young's moduli and Poisson's coefficients of the components were needed. Consequently, the displacement was incremented by 5.10^{-5} any 0.1 second until reaching the value of 0.0005 mm.

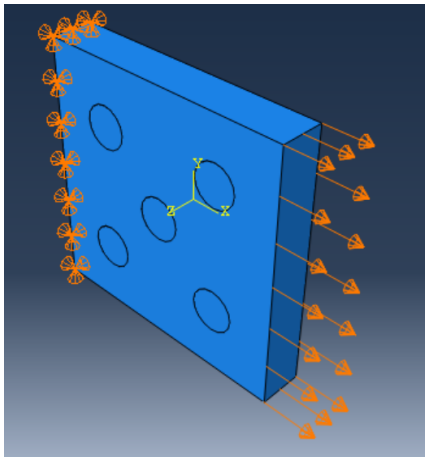

Figure 9: Figure of the applied displacement to measure transverse Young's modulus, and boundary conditions.

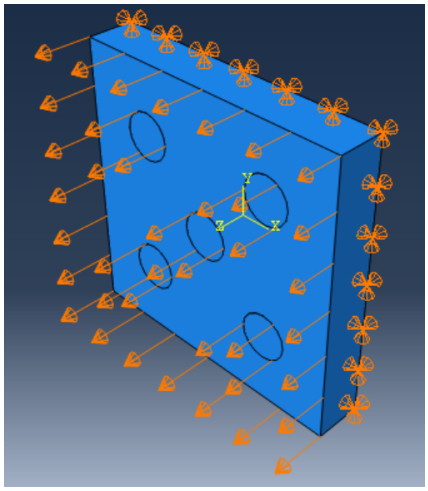

Figure 10: Figure of the applied displacement to measure axial Young's modulus, and boundary conditions.

About the meshing of the parts, C3D8R elements were used with linear geometric order. They are 8-node linear bricks that reduce integration. Global seeds for each part, that is to say for matrix and reinforcement, were used to specify the target mesh density. Mesh controls have been computed to specify the shape of the elements in the mesh. This was necessary to take into account the structure of the parts. To do so, the software transforms the mesh of a regularly shaped region, such as a square or a cube, onto the geometry of the region we want to mesh. This is the case with hexagonal-dominated element shape with sweep technique using medial axis algorithm as shown in figure 11.

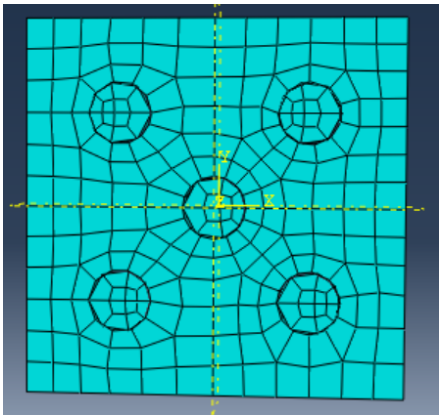

Figure 11: Figure of the meshed structure of the assembly with structured meshing in ABAQUS/FEA.

Then, global seeds were adapted in such a way that the total number of nodes does not exceed 1000 nodes, keeping in mind that the higher the number of nodes, the more accurate the results. Once the model submitted, results are presented.

The aim of mechanical analysis was to determine axial and transverse Young's moduli as said above. To do so, axial and transverse reaction forces were obtained with the output data base of the analysis for each unique nodal of the surface of applied displacement (surfaces with arrows in figure 9 and figure 10). Since each nodal of this surface is subjected to the same displacement amplitude, reaction forces at unique nodes were summed for each time increment, this sum was divided by the surface where was applied the displacement in order to obtain the corresponding stress. Then the displacement at each time increment was divided by the initial length of the material to obtain the strain, true strain and true stress were calculated to plot them on a graph and results were correlated.

- The study of the influence of the volume fraction of reinforcement has been carried out through three cases by varying the radius of short-fibers between 5.585% and 15.708% with the same material for short-fibers, which was TiB_2. Axial and transverse Young's moduli were

estimated thanks to Hooke's law and correlations between them and the fraction volume of reinforcement have been completed. Results were also compared of those obtained with the ROM (equation 4), IRM (equation 5) and Tsai-Halpin relation (equation 6).

- The study of the influence of the material used for reinforcement has been achieved by undertaking three types of intermetallics: TiB_2, ZrB_2 and CrB_2. The fraction volume of reinforcement was set at 15.708%. Young's moduli were also estimated thanks to Hooke's law and compared with those of the ROM and the IRM.

ii Thermal analysis

For this analysis, an aluminium-based metal matrix composite reinforced with a 15.708% of TiB_2 short-fibers was considered. Two sub-analysis were carried out: one in order to estimate axial and transverse coefficients of thermal expansion of the composite material, and another one to correlate thermal behaviour of the material with the Newton's law of heating. As opposed to the mechanical analysis, a time-dependant procedure has been set to analyze the time-dependent material response.

In both cases, an initial temperature was set to 293 K for the whole composite material. A temperature of 350 K is then applied on one face of the material and heat transfer is studied. Thus, since the maximal change in temperature is about 50 K, mechanical and thermal properties can be considered as temperature-independent in this interval. These faces are those in figure 9 and figure 10 where were applied boundary conditions. To study the mechanical and thermal behaviours of the material, a transient coupled temperature-displacement procedure was set up. That's why thermal properties such as specific heat capacity, density, CTE and thermal conductivity are required to carry out the procedure. Due to the very small dimensions of the composite material, the time period of the step is also very low, about 3 ms. In fact, the material being very small, steady-state is reached quickly.

The meshing procedure is the same as for the mechanical study. The only difference came with the type of meshing elements. Since a coupled temperature-displacement procedure was set, 8-node thermally coupled brick elements were used to mesh the parts and structure of the materials was also took into account. Following steps will be described subsequently for each analysis:

- Determination of axial and transverse CTEs was based on the mathematical expression of thermal expansion, which is represented in equation 13.

$$\epsilon_{thermal} = \alpha_L(T_{final} - T_{initial}) \tag{13}$$

Where $\epsilon_{thermal}$ is the thermal strain caused by thermal gradients and α_L is the linear thermal expansion coefficient. In our case, $T_{initial}$ is the predefined temperature of the material,

which was set to 293 K and T_{final} has been considered as the average temperature of the whole material at a time t. Thermal strain was also obtained, by calculating the average displacement at any node of the structure, for each time increment.

Output data of average displacement and average temperature were obtained for each time increment, then average strains for each time increment were calculated and strain vs ΔT was ploted to determine CTEs through lineal regressions. Results were compared to those obtained with equation 8 and equation 9. Finally, this approximations provide average values of axial and transverse linear CTEs.

- The thermal behaviour of the composite material was evaluated by measuring the average temperature at each node of the structure, for each time increment. Temperature vs time was ploted and results were compared to Newton's law of heating.

  Newton's law of heating models the average temperature in an object by a simple differential equation. Once solved, it provides an expression of the temperature, considered as uniform, in the material as a function of the time as shown in equation 14. Newton's law of heating assumes that the temperature of the object is represented by a single number.[39]

$$T(t) = T_\infty + (T_0 - T_\infty)e^{\frac{-t}{\tau}} \tag{14}$$

  Where T_∞ is the temperature of the material once steady-state reached, which is the temperature of 350 K imposed, T_0 is the initial temperature of the material, 293 K and k is the time-constant of the system. By solving the differential equation, we find that τ is equal to $\frac{C}{h.A}$ where h is the heat transfer coefficient of the material, A is the surface area of the body through which the heat is transferred, and C is the heat capacity of the material.[40]

  Thus, while heating, the temperature of the material exponentially approaches the temperature imposed to the surface. This law is valid for low temperature variations, that not exceed 200 °C or 300 °C. One other condition is that the internal thermal resistance within the object have to be smaller than the resistance to heat transfer away from the material surface. This is not really the case of our simulations because there is no heat transfer "away from the material", but it will be discussed in the results section.

4 Results and discussion

4.1 Mechanical behaviour

4.1.1 Influence of the volume fraction of reinforcement

In this first analysis, the Young's modulus of the composite material for three volume fraction compositions have been studied. Once reaction forces data obtained, true strain and true stress calculated, results were ploted. Correlations between true strain and true stress were conducted for each case, i.e. for each volume fraction in axial and transverse direction. Correlation coefficients are presented in table 5 below to highlight the representativeness of the results.

Table 5: Table of the correlation coefficients between true strain and true stress for each volume fraction of reinforcement, in axial and transverse directions.

Short-fiber composition	Axial correlation coefficient	Transverse correlation coefficient
5.585 %	0.998	0.995
9.4248 %	0.999	0.988
15.708 %	0.999	0.989

The graph coming from these simulations clearly shows the good agreement between experimental values and values calculated with usual rules as shown in figure 12:

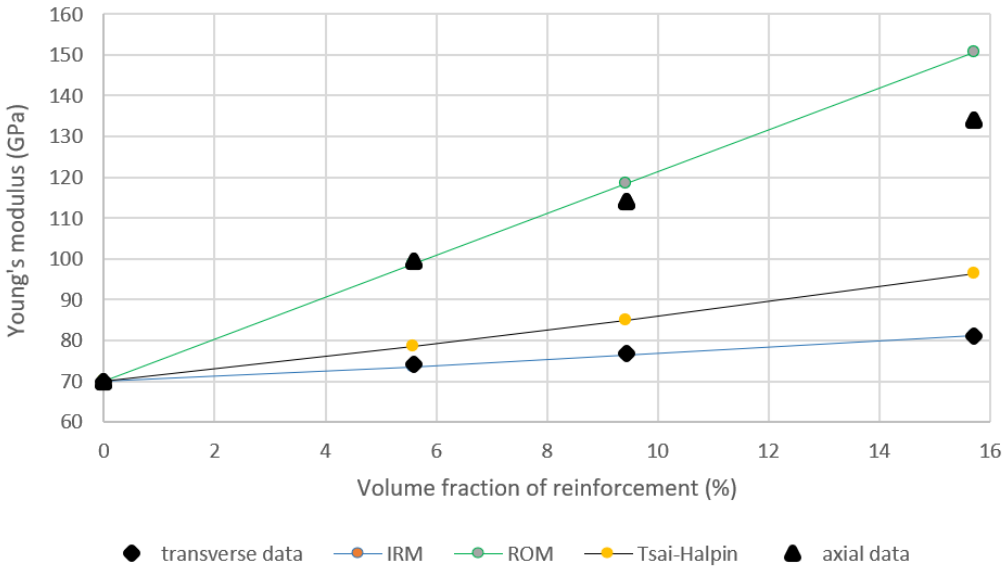

Figure 12: Comparison of theoretically calculated Young's modulus values with the experimentally determined values for short-fibers reinforced composite materials by varying its fraction content.

Firstly, data in table 5 shows that the linear correlation of true stress and true strain is significant. A strong linear relation exists between these two variables since correlation coefficients are very close to 1. Thus, Hooke's law is verified for this configurations, but this was partially expected due to the fact that only elastic behaviours of the components were input, no visco-plastic or elasto-plastic laws were computed either. Moreover, these correlation coefficients confirm the idea that displacement control was the wisest choice. The fact that each node of the front face were submitted to the same displacement increments make it possible to calculate the corresponding stress by summing reaction forces for each node, this method provided significant results.

About the results of figure 12, they confirm the good agreement between calculated and experimental values for axial and transverse directions. In fact, in the case of the transverse Young's modulus, data fit quasi-perfectly the theoretical lower bound of properties of the composite material i.e. stiffness values obtained with the IRM. For axial Young's modulus, data also fit well the upper curve of properties, obtained with the ROM, but the last experimental point differs more than the other one from ROM curve.

It is stated that Voigt model that models axial properties of fiber reinforced materials is only applicable for long-fiber reinforced composite materials as long as the dimensions of the matrix, but it seems to be also applicable for short-fibers reinforced materials, for a volume content of fiber up to 10 %. Voigt model adopted isostrain assumption to obtain the estimation of the effective composite stiffness, which is convenient with our simulations since we adopted displacement control. Thus, as it has already been said previously, for each time increment, each point of the front face, whether fiber or matrix, have the same strain.

Transverse stiffness values, meanwhile, perfectly fit the lower curve. The Reuss model that establishes the IRM is based on the the isostress assumption, that is to say that the applied global force is fully transmitted to the fibers and the matrix, the stresses in both the matrix and fibers are the same. Since reinforcement is used to carry out loads of the whole material, stresses of the matrix and the short-fibers are not equals, and transverse results must not be as close of the lower bound as they are. As depicted in figure 13, stresses along the x-axis are not equals between matrix and fibers. Even if differences are low, about 30 MPa between the center of a fiber and its surroundings, experimental stiffness must diverge from the IRM.

Another interesting point in figure 12 is that experimental transverse Young's moduli are closer with the lower curve than with the Tsai-Halpin curve, while dimensions of the fibers are taken into account in this model. This can be explained by the fact that Tsai-Halpin equation has been initially established to fit some experimental results at low-volume fractions. We could notice that until a volume content of 10 %, experimental data and those obtain with Tsai-Halpin model are not so far apart, and then the difference is more pronounced.

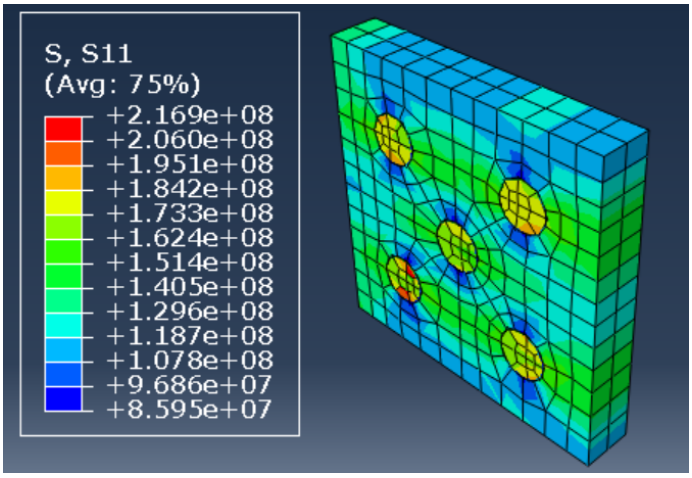

Figure 13: Representation of the differences in stress between matrix and short-fibers along x-axis

Correlations between Young's modulus and volume content of fibers provided a mathematical equation that significantly represents the relation between this two variables. This correlations is exposed in figure 14 below:

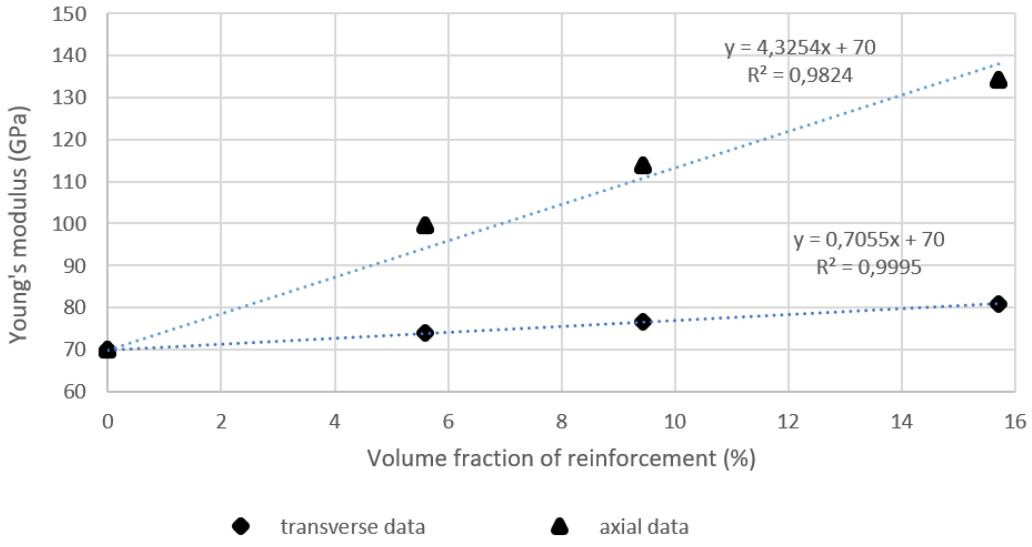

Figure 14: Correlation between Young's modulus and volume content of fibers in axial and transverse directions.

This correlations shows that, for a volume content of reinforcement lower than 15 %, the axial stiffness in increased of 4.3254 GPa per percent of fiber, and the transverse stiffness is increased of 0.7055 GPa per percent of fiber.

4.1.2 Influence of the nature of the intermetallic employed

We already know that Young's modulus of composite materials is mainly limited by the volume fraction of reinforcement, its stiffness, and matrix stiffness. Since we only considered in this study aluminium-based metal matrix, two parameters could be taken into account. The influence of the volume content of short-fibers has been investigated in the previous section. Now, the study will focus on the influence of the stiffness of the reinforcement employed. To do so, as said previously, three materials have been used as reinforcement. The main point of interest is their Young's modulus, that have been represented in x-axis in figure 15.

As for volume content influence, true strain and true stress were calculated and results were ploted. Correlations between true strain and true stress were conducted for each case, and very significant results have been obtained. In order to present results in the most appropriate way possible, I decided to represent axial and transverse Young's moduli as functions of the Young's modulus of short-fibers. Results are presented in figure 15 where values from ROM, IRM and Tsai-Halpin models are also ploted to compare with.

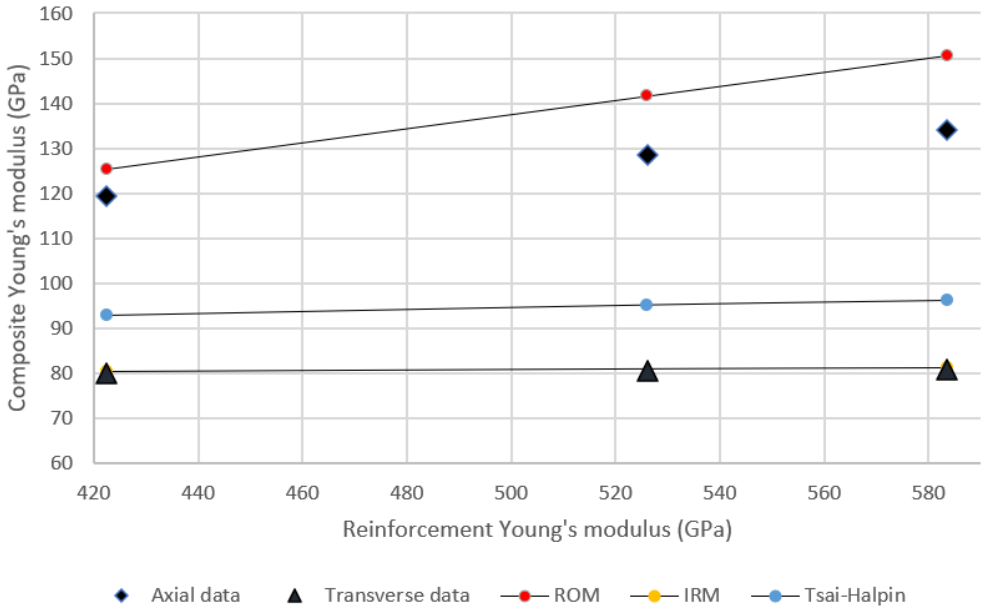

Figure 15: Comparison of theoretically calculated Young's modulus values with the experimentally determined values for short-fibers reinforced composite materials by varying stiffness of reinforcement.

In the same way as the previous analysis, transverse data fit very well data from the inverse rule of mixture, that's why points from this model are not discernible, they are hidden by experimental

transverse points. The difference of modulus obtained experimentally and with IRM does not exceed 1 GPa. Differences are more pronounced between experimental axial data and data from the rule of mixture. In the study of the influence of the volume content, it has been noticed that for a volume content of fiber up to 10 %, Voigt model was considered as valid. Above 10 %, we observed that results tended to diverge. Since the volume content for this study has been fix to 15,70 %, it seems to be logical that experimental data diverge from those of IRM. To confirm this trend, it would have been interesting to carry out same analysis, but with a lower volume fraction of short-fibers.

Linear regressions have been established for axial and transverse data, in order to provide an equation that governs the evolution of composite Young's moduli as a function of stiffness of the reinforcement. Results and regression coefficients are shown in figure 16.

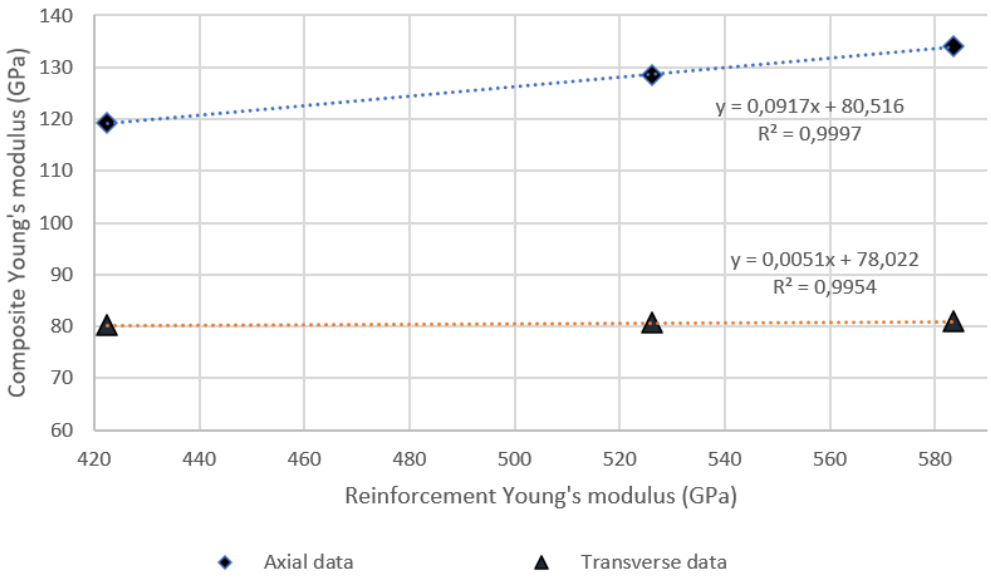

Figure 16: Correlation between composite Young's modulus and stiffness of fibers in axial and transverse directions.

Here, the y-intercept coefficient means nothing, because scale has been reduced in order to have a better view scale on results. By increasing the stiffness of the reinforcement of 1 GPa, we will also increase axial stiffness of 0.0917 GPa, and transverse stiffness of 0,0051 GPa.

To sum up this two mechanical analysis, it has been shown that the stiffer the reinforcement, the stiffer the composite material, but the increase of volume content also improves this stiffness. It constitutes a great stake at industrial scale. Since manufacture metal-based metal matrix composite is an expensive area, due to the costly processes, but also to the cost of materials used, sometimes very high. That's why a compromise is often made between volume ratio of reinforcement, and the

material used. Obviously, materials used as reinforcement not only determine the stiffness of the whole material, but also its strength, wear resistance, and more often its density. However, in some cases, it must be convenient, from an economic standpoint, to produce a composite material with a lower volume content of reinforcement, but with a stiffer material.

4.2 Thermal behaviour

4.2.1 Determination of coefficients of thermal expansion of the composite material.

Axial and transverse coefficients of thermal expansion have been determined thanks to equation 13. In the table 6 are presented values from equation 8 and equation 9 which provide theoretical values of axial and transverse CTE according to Schapery model.

Table 6: Table of axial and transverse CTEs using the experimental and theoretical axial Young's modulus of the composite material.

Young's modulus	$\alpha_{33,c}$	$\alpha_{11,c}$
Experimental E_c	$1.49.10^{-5}$	$2.34.10^{-5}$
Theoretical $E_c(fromROM)$	$1.33.10^{-5}$	$2.38.10^{-5}$

Experimental value of axial E_c providing from the study of the volume content of reinforcement, has been valued at 134.1 GPa. As discussed in 4.1.2, there is a difference between theoretical and experimental value of axial Young's modulus, resulting in a difference in axial and transverse CTEs using both values. Data output of average ΔT and average strain were obtained, and results ploted. Figure 17 and figure 18 present the linear regressions from experimental data for axial and transverse directions respectively. In comparison with equation 13, it comes that the slope coefficient corresponds to the average CTE corresponding. Since regression coefficients are very close to 1, values of coefficient can be considered as significant. Thus, we obtain $\alpha_{33,c} = 1.72.10^{-5}K^{-1}$ and $\alpha_{22,c} = 2.22.10^{-5}K^{-1}$.

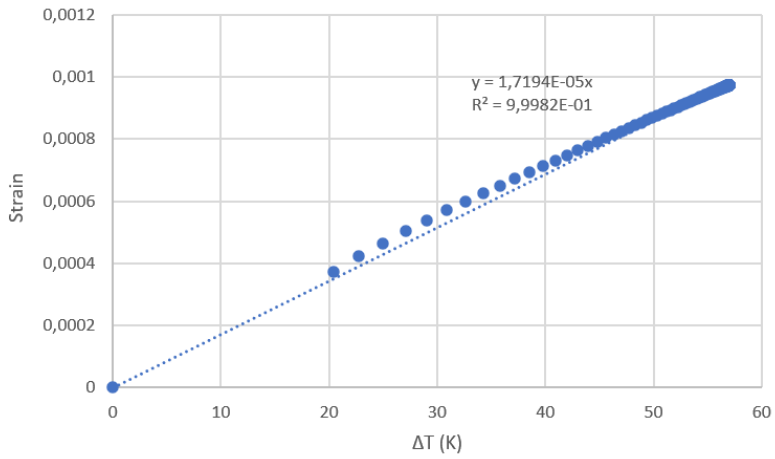

Figure 17: Correlation between average ΔT and average strain in axial direction.

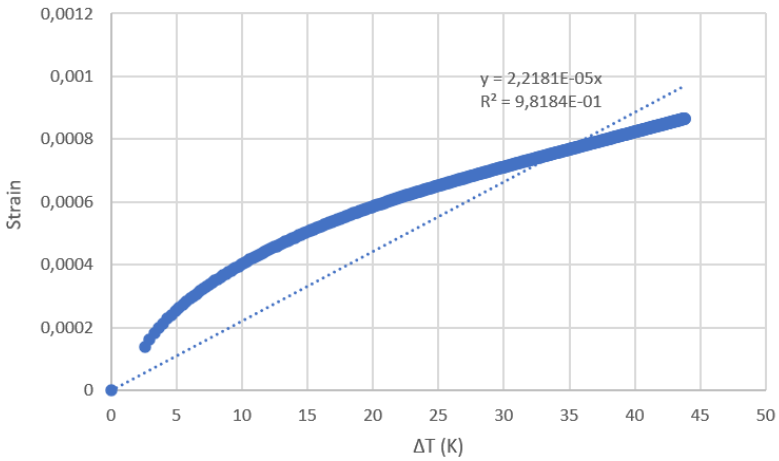

Figure 18: Correlation between average ΔT and average strain in transverse direction.

Firstly, we notice that experimental values are not that far from theoretical values, which means that numerical modelling are representatives of the real behaviour of the material. Table 7 presents the relative deviations between experimental and theoretical data. It shows that relative deviation is lower using experimental value of E_c. This may be due to the fact that analysis was carried out with the same computed model, same meshing features, same geometry and same properties. According to Schapery model, introduced in 1.2.2, and the influence of stiffness in the evolution of the coefficient of thermal expansion, the stiffness of the structure has been taken into account by the software.

Table 7: Table of the relative deviations between experimental and theoretical CTEs.

Young's modulus	$\alpha_{33,c}$	$\alpha_{11,c}$
Experimental E_c	15.44 %	5.12 %
Theoretical $E_c(fromROM)$	29.32 %	6.72 %

Nevertheless, as low as they may be, those deviations can be explicated by different points. Firstly, the bigger approximation made is the one of average strain. For each time increment, an average displacement based on the displacement of each nodes of the structure have been calculated, and divided by the initial length of the specimen. This average displacement could represent a point of the structure, but it surely does not match with a point whose initial position coincide with the initial length of the material.

Moreover, in order to make that the structure does not move away from its position, a boundary condition has been set on the bottom face of the material, by stopping any movement of the surface along x,y and z-axis, to "freeze" the structure. It generated stresses around the bottom surfaces, and affected displacement of node around the same surface. Probably that it has affected the calculus of average displacement at each time increment.

Despite all, results are representative. The findings of this analysis confirm the reduction in CTE by adding a second phase whose coefficient of thermal expansion is lower than the matrix. Obviously, the orientation of short-fibers also plays an important role on global CTE of the composite material. It would have also been interesting to study the variation of this coefficient by varying the fraction content of reinforcement, or varying the orientation of short-fibers, in order to obtain a material whose CTE could be considered as homogeneous in all directions.

4.2.2 Analysis of heating behaviours of the material

For this analysis, three cases have been considered to explore the influence of reinforcement dispersion into the matrix in heating behaviours of the composite material. To do so, an aluminium specimen, without reinforcement, have been modeled, as well as a TiB_2-homogeneously reinforced aluminium matrix, a TiB_2-vertical reinforced aluminium matrix and an TiB_2-horizontal reinforced aluminium matrix. The homogeneously reinforced material is that one on figure 9, horizontal and vertical reinforced materials are shown in figure 20 and figure 19 respectively to get a clearer idea of what it is. On this same figures, the red boxes on left-face represent the face where is applied the temperature of 350 K.

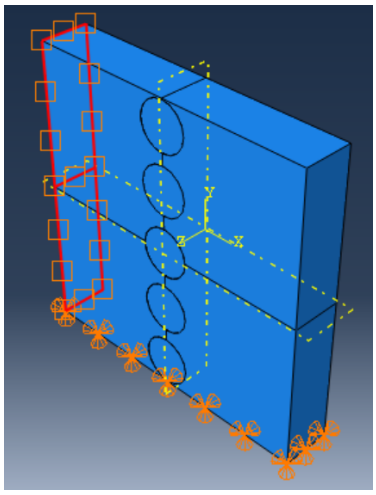

Figure 19: Figure of the vertical dispersion of reinforcement into the matrix (TiB_2-vert.Reinf.Al)

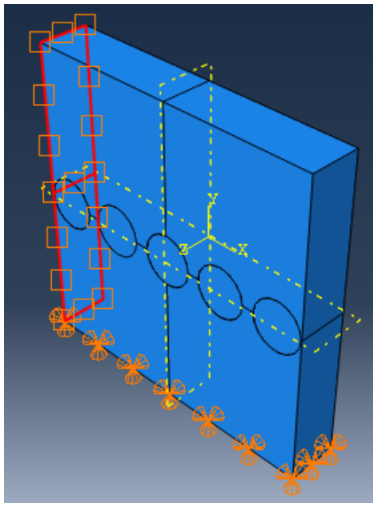

Figure 20: Figure of the horizontal dispersion of reinforcement into the matrix (TiB_2-horiz.Reinf.Al)

Dashed line planes represent symmetry planes, useful to establish the mesh the most adapted to the structure. Thus, average temperature at each time increment have been obtained thanks to output data, and ploted as function of time. Figure 21 presents results for each configuration.

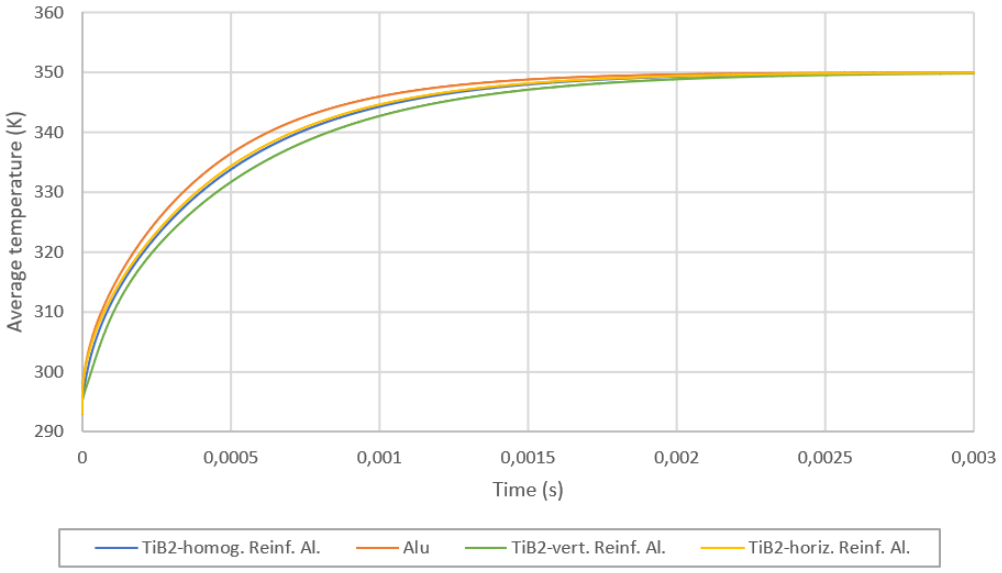

Figure 21: Evolution of the average temperature of the composite material as a function of time, for the four configurations.

Firstly, results clearly reveal an inverse exponential trend of the average temperature of the structure, that seems to converge to the applied temperature of 350 K. This trend is similarly to the one of Newton's law of heating in equation 14. When t tends towards infinity, the average temperature of the material tends to the temperature applied on left-face. Thus, we could suppose that data form the software could be approach by Newton's law, assuming the coefficients T_∞ and T_0. T_∞ is obtained when t tends toward infinity, graphically we read that $T_\infty = 350$ K. T_0 is obtained when t tends towards O, and we read $T_0 = 293$ K, the initial temperature of the material.

Moreover, we notice that steady-state in not reached simultaneously for all configurations. It is reached firstly by aluminium specimen ,and then by specimen reinforced with TiB_2. This is due to the fact that thermal conductivity of aluminium is higher than thermal conductivity of TiB_2. Since steady-state in not reached simultaneously for reinforced structure, it means that the configuration and dispersion of short-fibers affects thermal behaviours of the composite material.

To study these differences further in depth, a model has been developed based on Newton's law, assuming the coefficients as said above. Equation 14 has been linearized thanks to natural logarithm function. Linearized function is shown below:

$$ln(\frac{T - T_\infty}{T_0 - T_\infty}) = -\frac{t}{\tau} \tag{15}$$

$ln(\frac{T-T_\infty}{T_0-T_\infty})$ has been ploted below in figure 22 as a function of the time. Comparing with equation 15, slope coefficient corresponds to $\frac{-1}{\tau}$.

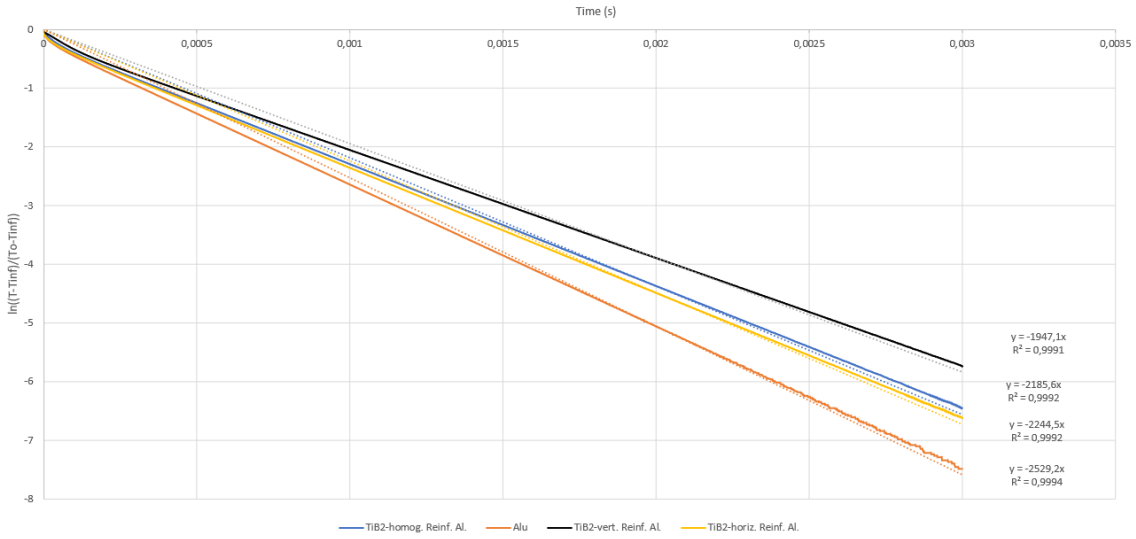

Figure 22: Evolution of the average temperature of the composite material as a function of time, for the four configurations.

For clarity, slope and regression coefficients are resumed in table 8 below. Since regressions are significant according to regression coefficients, time constants τ can be determined. These values are also presented in table 8.

Table 8: Table of the slope and regression coefficients from curves in figure 22.

Coefficient	TiB_2-homog. Reinf. Al.	Alu	TiB_2-vert. Reinf. Al.	TiB_2-horiz. Reinf. Al.
Slope coeff. (s^{-1})	-2185.6	-2529.2	-1947.1	-2244.5
Reg. coeff. R^2	0.9992	0.9994	0.9991	0.9992
τ (s)	$4.57.10^{-4}$	$3.95.10^{-4}$	$5.14.10^{-4}$	$4.46.10^{-4}$

Physically, this time constant τ represents the time period for which average temperature reaches the value T_∞ + (T_0 - T_∞).e^{-1}. In our case, this value is approximately about 329 K.

Thus, the higher the time constant, the lower the ability of the composite material to diffuse heat. Naturally, aluminium is the model whose time constant is the lower, steady-state is reached rapidly compared to other models. The fact that TiB_2, is considered as ultra-refractory ceramic material directly affects thermal behaviours by restricting the expansion of areas at very high temperatures through the composite material. In addition, dispersion of reinforcement into the matrix seems to also affects those thermal behaviours. In fact, for short-fibers dispersed vertically along y-axis, time constant τ is the highest among the four models. It is probably due to the fact that, according to figure 19, reinforcement constitutes a kind of "wall" that prevents heat from spreading. Homogeneous and horizontally-dispersed reinforcement models provide substantially identical values of time constant.

At industrial scale, a vertical dispersion into the matrix of particles or fibers could be achieved if reinforcement is electrically or magnetically active. The application of high electric and magnetic fields could orients particles or fibers along a specific axis into the molten matrix. Caution should be exercised if the molten matrix also reacts under action of magnetic fields.

Let's focus now on the great agreement of experimental data with Newton's law. It as been said in 3.2.2, ii that the internal thermal resistance within the object have to be smaller than the resistance to heat transfer away from the material surface. However, in our case, there is no transfer away from the material, the only heat transfer comes from the heated left-face of the specimen, and thus the heat transfer within the material is forced. Thus, there is no comparative form of heat transfer to internal thermal transfer, and this condition is automatically verified. However, this law is also verified if temperature within the material can be considered as homogeneous. Since we set that average temperature is the temperature in each node of the material, it is automatically verified. Nevertheless, it is clear that temperature gradient exists within the material at each time increment, and average temperature does not necessarily represent the real temperature at each node at a time t. Finally, this computed model gives an idea of the trends of the thermal behaviour

of such a material, but in reality results differ from them.

As said in previous sections, Newton's law set that time constant corresponds to $\frac{C}{h.A}$, where h is the heat transfer coefficient of the material, A is the surface area of the body through which the heat is transferred, and C is the heat capacity of the material. With the objective of increasing τ, there are three possibilities. Firstly, heat capacity of the material must be increased, by reinforcing the matrix with a material whose heat capacity by mass unit is higher than the one of the matrix. According to table 4 and table 3, heat capacity of the aluminium matrix is higher than the one of titanium diboride, which means that the amount of energy that must be added, in the form of heat, in order to cause an increase of one Kelvin is higher in the case of aluminium. In our case, this coefficient does not allow to increase time constant.

By reducing the heat transfer coefficient h, time constant can also be increased, and thus thermal behaviours of the composite material are improved. This coefficient is the proportionality constant between the heat flux and the thermodynamic driving force for the flow of heat, i.e. ΔT. In our case, this coefficient does not directly affects heat transfer because there is no convective heat transfer away from the surface of the material, but this coefficient is related to the thermal conductivity k through the dimensionless Nusselt number as shown below:

$$Nu = \frac{hL_c}{k} \tag{16}$$

Where h is the heat transfer coefficient, L_c is a characteristic length and k the thermal conductivity. Empirical correlations provide an equation for calculating the Nusselt number. Thus, by reducing thermal conductivity, we also contribute to reduce the heat transfer coefficient. Since, TiB_2 has a lower thermal conductivity than aluminium, is contributes to reduce τ. Reducing the surface area of the body through which the heat is transferred also increase time-constant, but it is highly limited by the material geometry, and its functions.

5 Conclusion

The main objective of this project was to characterize an aluminium-based metal matrix composite reinforced with intermetallics. Due to the actual situation, characterization by common laboratory methods could not be achieved. However the subject has been somewhat modified and redirected to a modelling analysis of the behaviours of such a material, conducted with the software ABAQUS/FEA®.

From the results obtained for analyzing the mechanical and thermal properties of this composite material, it can be summed up that:

- By increasing the volume fraction of short-fiber reinforcement, we linearly increase axial and transverse stiffness as the rule of mixture ans inverse rule of mixture predict. Due to the fact that in axial direction short-fibers are mechanically stressed along fiber direction, stiffness in this direction increases more than in transverse direction. In order to take advantage of fiber properties, fiber length must be such that the tensile load must be equal to the shear load supported by the fibre, and this equality provides a critical value of fiber length.

- About the influence of the nature of the intermetallic employed, results showed that the stiffer the intermetallic reinforcement, the stiffer the composite material. As set out in the introduction, intermetallics materials studied have a high Young's modulus compared to usual metal alloys. Depending on the field of application, compromises must be done between density and Young's modulus of material used as composite reinforcement. It is often considered that ceramic materials provide high Young's moduli, compared to metals, glasses or polymers, but in defiance to density. That's why compromises have to be made at the moment of selection of materials. But frequently, other properties are taken into account.

- Schapery model for the estimation of axial and transverse coefficients of thermal expansion provided values fairly close to experimental values obtained by simulations. Results highlighted the increased thermal stability of the composite material due to the reduced coefficients of thermal expansion in axial and transverse directions, even if difference is quite small in transverse direction, which provides an anisotropic or orthotropic material. This underlines the utility of multi-directional reinforcement for structure applications. Once more, experimental data fairly well agree with usual rules.

- It has been shown through simulations that reinforcing a material with refractory short-fibers also reinforces refractory behaviour of the whole composite material, depending on their dispersion within the matrix. This refractory behaviours of the whole material are related to thermal properties of reinforcement according to Newton's law, which should more or less guide the choice of materials for specific applications.

To sum up, intermetallics could represent an asset for industrial applications, both in terms of properties and manufacture processes. However their properties does not allow them for advanced applications such as aerospace applications. Materials such as alumina would be privileged due to their very low thermal conductivity, low density or low coefficient of thermal expansion.

6 Future work

In this part, discussions of the future work that could be done on this research will be done.

Firstly, since this project was only based on computer simulations, it would be convenient to compare the simulated results obtained to experimental results that could be obtained by many methods that were initially planned, such as ultrasonic techniques. Other characterization techniques such as microstructural analysis may also be realised to highlight other properties of such a material, that have not been studied with Abaqus.

Such properties could have been studied by implementing explicit models in Abaqus, which requires a better control of the software, that I don't have yet.

Moreover, so much other properties could have been studied such as ageing behaviours under dynamical loads, hardening processes, or plastic deformation in temperature or at constant temperature.

7 Budget

7.1 Introduction

The aim of this section is to establish the necessary cost to attain this project. Since no laboratory experiments were carried out, it is severely reduced and principally takes into account the direct cost, that is to say, the cost of the workforce. The amortization of computer hardware was also considered. It is true that student edition of the software ABAQUS/FEA®used is free for all students associated with an academic institution, but we will consider in this budget section that a professional version of the software has been used. It will be further detailed in 7.3.2.

7.2 Cost of the workforce

In this section, the workforce refers to my tutor, David Busquets, who has taken time to guide me, lead me and advise me throughout this project, and me. Costs considered are average costs based on the gross salary of professors and engineers in Spain. It has been considered the hourly cost of an engineer for the simulations I carried out and the data processing. Those data are resumed below:

Table 9: Table of the price of workforce.

Description	Unit Price (€/h)	Quantity (h)
Project tutor	45.00	10
Engineer	30.00	70

7.3 Cost of the material

7.3.1 Cost of the computer hardware

To estimate the cost of the computer hardware, its amortization has been considered thanks to equation 17 :

$$A = \frac{t.C}{T} \tag{17}$$

Where A is the amortization, t the time of utilisation of the laptop, T the amortization period, and C the cost of the laptop (*valued added tax* included).

The cost of the computer hardware was about 500 €, and the amortization period was estimated to four years, according to manufacturers. Approximately 150 hours were required to carry out simulations, build on the results and prepare the report. Thus, the amortization of the laptop have been estimated to 2.14 €.

7.3.2 Cost of the software

It is considered in this section that Abaqus professional edition, including Abaqus/Explicit, Abaqus/Standard and Abaqus/FEA, costs on average about 2000 € per month. There are many promotions that Dassault Systèmes can offer. Available promotions can run up-to 68 % off Abaqus, so there is no locked prices. Abaqus has three different licensing options as far as how to buy the software: quarterly or yearly lease, or the purchase of Abaqus. Thus, considering that simulations were carried out over a single month, it is quite realistic to consider an average cost of 2000 € of the software.

7.4 Global executive budget

Table 10: Table of the global executive budget of the project.

Description	Price (€)
Project tutor	450
Engineer	2100
Computer hardware	2.14
Software	2000
Total (€)	4 552.14

Finally, the global cost of this research project is four thousand five hundred fifty-two euros and fourteen cents / Cuatro mil quinientos cincuenta y dos euros y catorce céntimos.

References

[1] Rahul Reddy Nagavally. "Composite materials - history, types, fabrication techniques, advantages, and applications." In: *Proceedings of 29th IRF International Conference* (2016).

[2] Mar-Bal incorporated. *History of Composite Materials.* URL: https://www.mar-bal.com/language/en/applications/history-of-composites/. (accessed: 22.11.2020).

[3] *Anubis Mask from Harrogate - rear right view.* URL: https://en.wikipedia.org/wiki/Cartonnage#/media/File:Anubis_Mask_from_Harrogate_-_rear_right_view. (accessed: 22.11.2020).

[4] Ajith James Cyriac. "Metal matrix composites: history, status, factors and future". 2011.

[5] Suraj Rawal. "Metal-Matrix Composites for Space Applications". In: *JOM* (Apr. 2001), pp. 2–4.

[6] Yves Meshaka. "Matériaux Composites : Comportement mécanique tomes 1 et 2". In: Yves Meshaka, 2019. Chap. 1 and 2.

[7] Arun Kumar Sharma. "A study of advancement in application opportunities of aluminum metal matrix composites." In: *Elsevier* (Jan. 2020), pp. 2–6.

[8] Ori lshai Isaac M. Daniel. "Engineering mechanics of composite materials". In: *Oxford university press* (2006), pp. 17–53.

[9] P. S. Theocaris. "The Role of the Polymeric Matrix in the Processing and Structural Properties Composite Materials". In: Springer, 2015. Chap. 7.

[10] Karen S. Devens Robert M. Jones. *Mechanics of composite materials.* Library of congress cataloging-in-publication data. Taylor and Francis, 1999. ISBN: 1-56032-712-X.

[11] Karl Ulrich Kainer. "Basics of Metal Matrix Composites". In: 2006, pp. 1–54.

[12] K. S. Shivakumar Aradhya M.B. Vinod. "Validation of Halpin-Tsai and Nielson empirical relations for composite materials using finite element method." In: *50th Congress of ISTAM* (2005), pp. 1–9.

[13] S. I. Kundalwal. "Review on Modeling of Mechanical and Thermal Properties of Nano- and Micro-Composites". In: *Indian Institute of Technology* (2017), pp. 17–26.

[14] R. A. Schapery. "Thermal Expansion Coefficients of Composite Materials Based on Energy Principles". In: *Journal of composite materials* (1968), pp. 2–27.

[15] Amit Aherwar Arun Kumar Sharma Rakesh Bhandari. "Matrix materials used in composites: A comprehensive study". In: *Elsevier* (2019), pp. 1–4.

[16] Dayang Laila Mohd Nurazzi. "A Review: Fibres, Polymer Matrices and Composites". In: *Pertanika* (2017), pp. 4–18.

[17] *Metal-matrix composites.* URL: https://www.machinedesign.com/materials/article/21812641/metalmatrix-composites. (accessed: 25.11.2020).

[18] William A. Curtin. "Theory of Mechanical Properties of Ceramic-Matrix Composites". In: Journal of the American ceramic society, 1991, pp. 2837–2845.

[19] I.M Low. "Ceramic-Matrix Composites: Microstructure, Properties and Applications". In: Woodhead publishing, 2006, pp. 99–128.

[20] Jianhong Gao Li Hong Huang Xiaoxiang Yang. "Study on Microstructure Effect of Carbon Black Particles in Filled Rubber Composites". In: *International Journal of Polymer Science* (2018), pp. 1–3.

[21] *Les nouvelles fontes GS à matrice ferritique renforcée font le show !* URL: `https://metalblog.ctif.com/2017/09/01`. (accessed: 29.11.2020).

[22] B.Harris A.R.Bunsell. "Hybrid carbon and glass fibre composites, Composites, Volume 5, Issue 4," in: 1974, pp. 157–164.

[23] *An introduction to Metal Fiber Technology.* URL: `https://www.bekaert.com/en/product-catalog/content/Metal-fibers/metal-fiber-technology-whitepaper-download-new`. (accessed: 10.12.2020).

[24] Rupa Dasgupta. "Aluminium Alloy-Based Metal Matrix Composites: A Potential Material for Wear Resistant Applications". In: *Advanced Materials and Processes Research Institute* (2012), pp. 1–5.

[25] *Intermetallic Phases Materials.* URL: `https://www.mpie.de/4129727/intermetallic-phases-materials`. (accessed: 13.12.2020).

[26] *Composé intermétallique.* URL: `https://fr.wikipedia.org/wiki/Compose%20intermetallique`. (accessed: 13.12.2020).

[27] M. Adamiak. "Selected properties of the aluminium alloy base composites reinforced with intermetallic particles". In: *Journal of Achievements in Materials and Manufacturing Engineering* (2005), pp. 1–5.

[28] R.A. Varin. "Intermetallic-Reinforced Light-Metal Matrix In-Situ Composites". In: *Metallurgical and Materials Transactions A* (2002), pp. 193–200.

[29] Hari Singh Bhaskar Chandra Kandpal Jatinder Kumar. "Production Technologies of Metal Matrix Composite: A Review". In: *International Journal of Research in Mechanical Engineering Technology* (2014), pp. 1–6.

[30] ZheChen Mingliang Wang DongChen. "Mechanical properties of in-situ TiB2/A356composites". In: *ElSevier* (2014), pp. 1–6.

[31] N. Shenbaga Vinayaga Moorthi S. Suresh. "Aluminium-titanium diboride (Al-TiB2) metal matrix composites: challenges and opportunities". In: *ElSevier* (2012), pp. 89–97.

[32] I. Dinaharan J. David Raja Selvam. "In situ formation of ZrB2 particulates and their influence on microstructure and tensile behavior of AA7075 aluminum matrix composites". In: *ElSevier* (2016), pp. 187–196.

[33] M. Gupta S. Lakshmi L. Lu. "In situ preparation of TiB2 reinforced Al based composites". In: *ElSevier* (1998), pp. 160–166.

[34] Ahmet Karaaslan Gokhan Ozer. "Properties of AA7075 aluminum alloy in aging and retrogression and reaging process". In: *ElSevier* (2017), 23572362.

[35] Peter N. Quested Juan J. Valencia. "Thermophysical Properties". In: *ASM Internationa* (2013), pp. 468–481.

[36] Katsushi Tanaka Norihiko L. Okamoto Misato Kusakari. "Anisotropic elastic constants and thermal expansivities in monocrystal CrB_2, TiB_2, and ZrB_2". In: *ElSevier* (2010), pp. 76–84.

[37] A. K. Suri B. Basu G. B. Raju. "Processing and properties of monolithic TiB_2 based materials". In: *International Materials Reviews* (2006), pp. 352–374.

[38] *ABAQUS/CAE*. URL: `https://www.3ds.com/products-services/simulia/products/abaqus/abaquscae/`. (accessed: 17.12.2020).

[39] Kristin Schmidtke Mark Gockenbach. "Newton's law of heating and the heat equation". In: *Involve* (2009), pp. 419–439.

[40] *Newton's Law of Cooling*. URL: `https://www.math24.net/newtons-law-cooling/`. (accessed: 19.12.2020).